Post-transcriptional gene regulation by the RNA binding protein IGF2BP3 is critical for MLL-AF4 mediated leukemogenesis

Tiffany M Tran[1,2], Julia Philipp[3], Jaspal Bassi[1], Neha Nibber[1], Jolene Draper[3], Tasha Lin[4,5], Jayanth Kumar Palanichamy[1,6], Amit Kumar Jaiswal[1], Oscar Silva[7], May Paing[1], Jennifer King[8], Sol Katzman[3], Jeremy R. Sanford[3], Dinesh S. Rao[1,2,9,10,11*]

[1] Department of Pathology and Laboratory Medicine, David Geffen School of Medicine at UCLA, Los Angeles, California, USA.
[2] Molecular, Cellular and Integrative Physiology Graduate Program, UCLA, Los Angeles, California, 90095, USA.
[3]Department of Molecular, Cellular and Developmental Biology, UCSC, Santa Cruz, California, 95064, USA.
[4]Division of Hematology/Oncology, Department of Medicine at UCLA, Los Angeles, California, 90095, USA.
[5] Molecular Biology Graduate Program, UCLA, Los Angeles, California, 90095, USA.
[6]Department of Biochemistry, All India Institute of Medical Sciences, New Delhi, 110029, India
[7]Department of Pathology, Stanford University School of Medicine, Stanford, California, 94305, USA.
[8]Division of Rheumatology, Department of Medicine at UCLA, Los Angeles, California, 90095, USA.
[9]Jonsson Comprehensive Cancer Center (JCCC) and
[10]Broad Stem Cell Research Center, UCLA, Los Angeles, California, 90095, USA.
[11]Lead Contact
*Correspondence: DRao@mednet.ucla.edu

Conflict of interest statement: The authors declare no competing interests.

ABSTRACT

Despite recent advances in therapeutic approaches, patients with MLL-rearranged leukemia still have poor outcomes and a high risk of relapse. Here, we found that MLL-AF4, the most common MLL fusion protein in patients, transcriptionally induces IGF2BP3 and that IGF2BP3 strongly amplifies MLL-Af4 mediated leukemogenesis. Deletion of *Igf2bp3* significantly increases the survival of mice with MLL-Af4 driven leukemia and greatly attenuates disease, with a minimal impact on baseline hematopoiesis. At the cellular level, MLL-Af4 leukemia-initiating cells require *Igf2bp3* for their function in leukemogenesis. eCLIP and transcriptome analysis of MLL-Af4 transformed stem and progenitor cells and MLL-Af4 bulk leukemia cells reveals a complex IGF2BP3-regulated post-transcriptional operon governing leukemia cell survival and proliferation. Regulated mRNA targets include important leukemogenic genes such as those in the *Hoxa* locus and numerous genes within the Ras signaling pathway. Together, our findings show that IGF2BP3 is an essential positive regulator of MLL-AF4 mediated leukemogenesis and represents an attractive therapeutic target in this disease.

INTRODUCTION

Chromosomal rearrangements of the mixed-lineage leukemia (*MLL*, also known as *KMT2A*) gene are recurrently found in a subset of acute lymphoblastic leukemia (ALL), acute myeloid leukemia (AML), and in acute leukemia of ambiguous lineage (Krivtsov and Armstrong, 2007). Despite recent advances in therapeutic approaches, patients with *MLL*-rearranged (MLLr) leukemia have very poor outcomes, a high risk of relapse, and show resistance to novel targeted therapies (Moorman et al., 2010; Pui et al., 2011) (Haddox et al., 2017; Rayes et al., 2016; Wei et al., 2008). *MLL* encodes a H3K4 methyltransferase that has been shown to be required for hematopoietic stem cell (HSC) development during both embryonic and adult hematopoiesis (Ernst et al., 2004a; Jude et al., 2007). Many of the translocation partners for *MLL*, including *AF4 (AFF1),* encode proteins that regulate transcriptional elongation (Lin et al., 2010; Mohan et al., 2010; Smith et al., 2011). Of more than 90 translocation fusion partner genes, *MLL-AF4* (*KMT2A-AFF1*) is the most common *MLL* fusion protein in patients (Meyer et al., 2018). Biologically, *MLL-AF4*-driven leukemia is a distinct entity, with a unique gene expression profile showing significant overlap with stem cell programs (Krivtsov et al., 2008; Somervaille et al., 2009).

At the post-transcriptional level, emerging evidence suggests a role for microRNAs, RNA-binding proteins, and other novel mechanisms in regulating gene expression during leukemogenesis (Ennajdaoui et al., 2016; Jønson et al., 2014; Nguyen et al., 2014; Palanichamy et al., 2016; Park et al., 2015). We recently identified the oncofetal RNA binding protein (RBP) Insulin like growth factor 2 mRNA binding protein 3 (IGF2BP3) as an important regulator of gene expression in *MLL*-rearranged B-ALL (Palanichamy et al., 2016). IGF2BP3 is expressed during embryogenesis, lowly expressed in healthy adult tissues, and strongly re-expressed in cancer cells (Mueller et al., 2003; Mueller-Pillasch et al., 1999). Several studies have shown that elevated levels of IGF2BP3 expression are correlated with diminished patient survival in many cancer types and may be a marker of disease aggressiveness in B-ALL (Kobel et al., 2009; Lochhead et al., 2012; Schaeffer et al., 2010; Stoskus et al., 2011). Previously, we determined that overexpression

of IGF2BP3 in the bone marrow (BM) of mice leads to a pathologic expansion of hematopoietic stem and progenitor cells (HSPC), in a manner dependent on RNA binding. IGF2BP3 interacts primarily with the 3'UTR of its target transcripts, as with MYC and CDK6, resulting in an upregulation of transcript and protein (Palanichamy et al., 2016). In the case of MYC and CDK6, IGF2BP3 binding resulted in upregulation of target transcript and protein, with attendant effects on pathologic hematopoietic stem and progenitor cell expansion. Together, these studies illuminated a novel role for post-transcriptional gene regulation in the pathologic proliferation of HSPCs.

Experimentally, MLL-AF4 driven leukemogenesis has been studied using a range of *in vitro* and *in vivo* models leading to significant progress in our understanding of MLL-rearranged leukemia (Bursen et al., 2010; Chen et al., 2006; Krivtsov et al., 2008; Metzler et al., 2006; Montes et al., 2011; Tamai et al., 2011). Here, we explicitly tested the requirement for *Igf2bp3* in a bona-fide *in vivo* model of MLL-Af4 driven leukemogenesis (Lin et al., 2016). Deletion of *Igf2bp3* significantly increased the survival of MLL-Af4 transplanted mice and decreased the numbers and self-renewal capacity of MLL-Af4 leukemia-initiating cells (LICs). Mechanistically, we found that IGF2BP3 targets and modulates the expression of transcripts within the *Hoxa* locus and components of the Ras signaling pathway, both key regulators of leukemogenesis, through multiple post-transcriptional mechanisms (Downward, 2003; Milne et al., 2010). Together, our findings show that IGF2BP3 is a critical regulator of MLL-AF4 mediated leukemogenesis and a potential therapeutic target in this disease (Downward, 2003; Milne et al., 2010).

RESULTS

The MLL-AF4 fusion protein transcriptionally induces IGF2BP3

To determine the functional impact of IGF2BP3 expression on MLL-AF4-mediated gene expression, we compared IGF2BP3-regulated targets with a published dataset of MLL-Af4 targets obtained by ChIP-Seq (Lin et al., 2016; Palanichamy et al., 2016). Transcripts modulated by IGF2BP3 were significantly enriched for MLL-Af4-bound genes (Figure 1A; Supplemental Figure 1A). Interestingly, IGF2BP3 itself was a direct transcriptional target of MLL-Af4, with binding sites within the first intron and promoter region of IGF2BP3 (Lin et al., 2016). To confirm if *IGF2BP3* was a direct transcriptional target of MLL-AF4, we performed ChIP-PCR assays on RS4;11 and SEM cell lines, human B-ALL cell lines that contain the MLL-AF4 translocation, and determined that a region in the first intron of *IGF2BP3* is strongly bound by MLL-AF4 (Figure 1B; Supplemental Figure 1B) (Wilkinson et al., 2013). This MLL-AF4 binding was abrogated when SEM cells were treated with the bromodomain inhibitor, iBET-151 (Supplemental Figure 1C) (Dawson et al., 2011). Furthermore, we observed an MLL-AF4-dose-dependent increase in luciferase reporter activity, using a 950bp promoter region upstream of the transcription start site (TSS) of IGF2BP3 (Figure 1C). To confirm that MLL-AF4 not only binds to the *IGF2BP3* gene but also promotes its expression, we utilized a retroviral MSCV vector encoding the human *MLL* fused to the murine *Af4* (MLL-Af4)(Lin et al., 2016). In the murine pre-B cell line, 70Z/3, and primary murine bone marrow cells, we found that MLL-Af4 transduction caused an approximately 64-fold upregulation of *Igf2bp3* mRNA (Figure 1D-E). Concordantly, IGF2BP3 protein was upregulated in MLL-Af4 transduced primary bone marrow cells, after being undetectable in control cells (Figure 1F). Taken together, these findings demonstrate that MLL-Af4 drives the expression of *Igf2bp3 in vivo*.

Normal hematopoiesis is maintained in Igf2bp3 KO mice

To test the *in vivo* requirement for IGF2BP3 in leukemogenesis, we generated an *Igf2bp3* KO (I3KO) mouse. We initially generated a floxed *Igf2bp3* allele (f/f; Supplemental Figure 2A)

using CRISPR/Cas9. In the course of mating the mice with the Vav1-Cre mouse strain, we serendipitously generated a germline knockout allele (del), which we isolated and further characterized (Supplemental Figure 2B). This generation of a germline knockout allele is consistent with prior reports for the Vav1-Cre mouse strain, which displays “leaky” Cre expression resulting in germline deletion (Croker et al., 2004; de Boer et al., 2003; Georgiades et al., 2002; Heffner et al., 2012; Joseph et al., 2013). Mendelian inheritance was confirmed, although the distribution of genotypes was marginally skewed (Table S1). Deletion of *Igf2bp3* was confirmed at the DNA, RNA, and protein level (Supplemental Figure 2C-E). Thus, *Igf2bp3*$^{del/del}$ (I3KO) mice were used for the remainder of the study. Immunophenotyping of I3KO mice showed no significant differences in the numbers of HSPCs in the BM compared to WT (Supplemental Figure 2F). Additionally, I3KO mice showed similar numbers of myeloid-lineage progenitors (including CMPs, GMPs, and MEPs)(Supplemental Figure 2G) and normal B-cell development as assessed by the Hardy scheme (Hardy and Hayakawa, 2001) (Supplemental Figure 2H) and normal numbers of mature B-lymphoid, T-lymphoid, and myeloid lineages in the BM and spleen (Supplemental Figure 2I-J). Hence, I3KO mice demonstrate preserved normal, steady-state adult hematopoiesis, although specific differences in other hematopoiesis conditions need further investigation.

Igf2bp3 deletion increases the latency of MLL-Af4 leukemia and survival of mice

After confirmation of preserved baseline hematopoiesis in I3KO mice, we next utilized bone marrow transplantation (BMT) assays to query MLL-Af4 mediated leukemogenesis (Supplemental Figure 3A). Retroviral MLL-Af4 transduction was equivalent between WT and I3KO donor BM, based on DNA copy number analysis (Supplemental Figure 3B) and Western blot analysis for MLL-Af4 (Supplemental Figure 3C). Following transplantation of the transduced HSPCs, we found that the loss of *Igf2bp3* significantly increases both the leukemia-free and overall survival of MLL-Af4 mice (Figure 2A-B). The median survival of WT/MLL-Af4 mice was

103 days while I3KO/MLL-Af4 mice had a median survival of greater than 157 days. Complete blood counts of WT/MLL-Af4 mice showed a consistent increase in WBC and absolute myeloid counts over time, which was severely blunted in I3KO/MLL-Af4 mice (Figure 2C; Supplemental Figure 3D). On average, peripheral blood counts crossed the leukemic threshold much earlier in WT/MLL-Af4 mice compared to I3KO/MLL-Af4 mice (70 days versus 112 days) (Figure 2C). Concordantly, peripheral blood smears showed reduced circulating blasts in I3KO/MLL-Af4 mice versus WT/MLL-Af4 mice (Supplemental Figure 3E). Together, these findings indicated that *Igf2bp3* is required for efficient MLL-Af4-mediated leukemogenesis.

Igf2bp3 modulates disease severity in MLL-Af4-driven leukemia

The MLL-Af4 model utilized here causes a highly penetrant, aggressive form of leukemia in mice. To characterize the role of *Igf2bp3* in disease severity, we performed detailed immunophenotypic and histopathologic analyses in MLL-Af4-transplanted mice in timed experiments. I3KO/MLL-Af4 transplanted mice showed a highly significant, approximately 4-fold reduction in spleen weights at 14 weeks post-transplant compared to WT/MLL-Af4 transplanted mice (Figure 2D). We observed near-total infiltration of the spleen and liver by leukemic cells, obliterating the normal tissue architecture in WT/MLL-Af4 mice, a finding that was much reduced in I3KO/MLL-Af4 mice (Figure 2E). In line with this, I3KO/MLL-Af4 transplanted mice showed a significant reduction in CD11b+ cells (Figure 2G; Supplemental Figure 3G), which were less proliferative (CD11b+Ki-67+), both in the spleen (approximately 30-fold) and in the BM (approximately 2.5-fold) at 14 weeks (Figure 2F; Supplemental Figure 3F). Thus, *Igf2bp3* deletion significantly reduces the tumor burden and attenuates disease severity in MLL-Af4 transplanted mice.

Igf2bp3 is required for LIC function in vitro

Several studies highlight the importance of LICs in both human and mouse leukemia. In the MLL-Af4 model, these LICs show expression of CD11b and c-Kit (Lin et al., 2017; Somervaille and Cleary, 2006; Somervaille et al., 2009). Given our findings of delayed initiation and decreased disease severity, we characterized these LICs, and found that I3KO/MLL-Af4 transplanted mice showed a significant 10-fold decrease in the numbers of leukemia-initiating cells (CD11b+c-Kit+) in the spleen and a 5-fold decrease in the BM at 14 weeks compared to WT/MLL-Af4 mice (Figure 3A-B). To further characterize the MLL-Af4 LIC and its dependence on IGF2BP3, we turned to endpoint colony formation assays. Utilizing immortalized HSPCs, denoted as Lin-, from WT/MLL-Af4 and I3KO/MLL-Af4 mice, we confirmed of equal transcript expression levels of MLL-Af4 and deletion of IGF2BP3 at the protein level (Figure 3C; Supplemental Figure 5A-B). The deletion of *Igf2bp3* resulted in an approximately 2-fold reduction in total colony formation as well as a significant decrease in CFU-GM progenitors (Figure 3D). To confirm our findings regarding LICs, we utilized an orthogonal method to delete *Igf2bp3* via CRISPR-Cas9. Briefly, Lin- cells from Cas9-GFP BL/6 mice were collected and transduced with the retroviral MSCV-MLL-Af4 vector. After selection, these MLL-Af4 Cas9-GFP Lin- cells were transduced with a retroviral vector with an mCherry fluorescence marker containing either a non-targeting (NT) sgRNA or a sgRNA targeted against *Igf2bp3* (I3sg) (Figure 3E). Importantly, *Igf2bp3* is deleted after transformation with MLL-Af4, a distinction from the previous method. After confirmation of *Igf2bp3* deletion (Figure 3F-G), GFP+mCherry+ MLL-Af4 Lin- cells were utilized for colony-forming assays. We confirmed that CRISPR-Cas9 mediated deletion of *Igf2bp3* led to a significant reduction in total colony numbers and decreases in the various colony morphologies (Figure 3H). The observed differences in overall colony forming capacity between the two systems are most likely a result of the different methodologies being used, but in both systems, IGF2P3 deficiency led to decreased colony formation. Thus, *Igf2bp3* is required for MLL-Af4 LIC function *in vitro*.

Igf2bp3 is necessary for the function of _MLL-Af4_ leukemia-initiating cells _in vivo_

Since *Igf2bp3* deletion causes a reduction in LICs and is required for the function of these LICs, we next wanted to determine if *Igf2bp3* specifically affects the capability of these LICs to initiate MLL-Af4 leukemia *in vivo*. First, to investigate baseline hematopoietic stem cell function in I3KO mice, we completed a competitive repopulation bone marrow transplantation experiment by transplanting lethally irradiated CD45.1 recipient mice with 50% of either WT or I3KO CD45.2 donor BM and 50% CD45.1 donor BM. We found no defect in engraftment over time in transplant recipients of I3KO BM (Supplemental Figure 4A). Moreover, we determined no differences in multilineage hematopoietic reconstitution ability of I3KO donor cells, as immature lineages in the BM and mature B-hematopoietic cells in the periphery were intact (Supplemental Figure 4B-H, respectively). Given that there were no baseline differences in reconstitution by normal HSPCs, we now sought to determine if *Igf2bp3* impacted the number of effective LICs in secondary transplant assays. We isolated BM cells from WT/MLL-Af4 and I3KO/MLL-Af4 mice with equivalent disease burdens and transplanted equal numbers (10^6, 10^5, and 10^4) of leukemic BM cells into immunocompetent CD45.1 mice. At 4 weeks post-transplantation, mice that received 10^6 cells from I3KO/MLL-Af4 mice had significantly reduced donor CD45.2+ cell engraftment (Figure 4A). With 10^5 and 10^4 transplanted cells, we no longer observed measurable leukemic burden in recipient mice (Figure 4A). This suggests that the active cell frequency of LICs in I3KO/MLL-Af4 mice is lost between 10^6 and 10^5 cells (Figure 4A)(Brien et al., 2010). Moreover, WBC and splenic weights were significantly decreased in I3KO/MLL-Af4 leukemia transplanted mice (Figure 4B-D). Histologically, leukemic infiltration was absent in the spleen and liver of 10^5 transplanted I3KO/MLL-Af4 mice (Figure 4E). Thus, *Igf2bp3* deletion greatly attenuated transplantability, in which only 17% of I3KO/MLL-Af4 recipients developed leukemia while 67% of WT/MLL-Af4 recipients developed leukemia at 4 weeks with 10^6 transplanted cells (Figure 4B). These data show that the deletion of *Igf2bp3* results in the significant reduction of LICs and reconstitution of MLL-Af4 transplanted mice, suggesting that *Igf2bp3* is necessary for the self-renewal capability of LICs *in vivo*.

IGF2BP3 supports oncogenic gene expression networks in LIC-enriched and bulk leukemia cells

To identify differentially expressed transcripts related to the I3KO phenotype, we sequenced RNA from WT/MLL-Af4 and I3KO/MLL-Af4 Lin- and CD11b+ bulk leukemia cells (Figure 5A-B, respectively). First, we confirmed expression of MLL and *Igf2bp3* in these samples by RT-qPCR and WB (Figure 3C; Supplemental Figure 5A-E). Differential expression analysis by DEseq2 revealed hundreds of differentially expressed transcripts (Figure 5A-B; Tables S2 and S3) (Love et al., 2014). We observed 208 upregulated and 418 downregulated transcripts in the CD11b+ cells, and 189 upregulated and 172 downregulated transcripts in the Lin- cells. To identify over-represented pathways and gene ontology terms within IGF2BP3 differentially regulated transcripts, we used the Metascape analysis tool (Zhou et al., 2019) and observed a significant enrichment in transcripts associated with the KEGG term related to transcriptional misregulation in cancer in both the Lin- and CD11b+ bulk leukemia dataset (Figure 5C-D). Interestingly, there were also distinct oncogenic networks that were regulated in the two datasets, with regulation of discrete signaling pathways noted in the Lin- cells (PI3K/AKT) and in the CD11b+ cells (GTPase, MAPK pathway) (Figure 5C-D). This was also confirmed by an independent analysis of differentially expressed data using GSEA, where we noted that the Hallmark KRAS pathway was significantly enriched in the CD11b+ cells (Supplemental Figure 5G) and GO oxidative phosphorylation in the Lin- cells (Supplemental Figure 5H). We used RT-qPCR to validate the RNA-seq data from both Lin- and CD11b+ cells. In Lin- cells, we focused on differentially regulated genes with a known leukemogenic function including *Csf2rb, Notch1*, *Cd69,* and the *Hoxa* cluster of transcripts, including *Hoxa9*, *Hoxa10, Hoxa7*. We observed a significant decrease in the steady state mRNA levels for each of these transcripts in the I3KO/MLL-Af4 Lin- cells, confirming our RNA sequencing results (Figure 5E). In CD11b+ cells, we selected transcripts known to play a role in Ras signaling, *Ccnd1*, *Maf*, *Mafb Itga6, Klf4, and Akt3* (Brundage et al., 2014; Eychène et al., 2008; Lewis et al., 2019; Riverso et al., 2017; Takata et al., 2005; Wagle et

al., 2018; Wu et al., 2019). As expected, these transcripts were decreased in I3KO/MLL-Af4 CD11b+ cells by RT-qPCR, confirming the high throughput RNA sequencing findings (Figure 5F). Furthermore, we determined that there was a significant decrease in Ras GTPase activity in the I3KO/MLL-Af4 CD11b+ cells compared to WT/MLL-Af4 CD11b+ bulk leukemia cells by ELISA assay (Figure 5G). Together, this data demonstrates that IGF2BP3 plays a major role in amplifying the expression of many cancer-related genes in Lin- and CD11b+ cells.

eCLIP analysis reveals a putative role for IGF2BP3 in pre-mRNA splicing

To determine how IGF2BP3 modulates gene expression in MLL-Af4 leukemia, we performed eCLIP to identify IGF2BP3 bound transcripts in both Lin- and CD11b+ cells (Figure 5A-B; eCLIP target transcripts denoted in red). Sequencing libraries were prepared from a minimum of two biological replicates with two technical replicates (four immunoprecipitations per cell line) as well as size matched input (smInput) samples from each condition. After filtering out reads that overlap the smInput, reproducible peaks were identified by using CLIPper (Tables S2-3; FS1 column) (Lovci et al., 2013). A significant fraction of the differentially expressed mRNAs are bound by IGF2BP3 ($P < 2.2x10^{-16}$; Supplemental Figure 6A). Motif analysis revealed an enrichment of CA-rich elements as expected (Supplemental Figure 6B) (Schneider et al., 2019). Although the majority of peaks were present within introns, we observed cell type-specific differences in the locations of IGF2BP3 binding sites within exons. In CD11b+ cells, a greater proportion of exonic peaks were found in 3'UTRs whereas a greater proportion of peaks mapped to internal exons in Lin- cells (Figure 6A). The eCLIP data revealed numerous peaks within precursor mRNA (pre-mRNA) in both Lin- and CD11b+ cells, suggesting a potential role in splicing regulation. To characterize this observation, we utilized MISO (Mixture of Isoforms) analysis to identify differentially spliced transcripts in WT/MLL-Af4 and I3KO/MLL-Af4 cells (Katz et al., 2010). Across both cell lines, we identified hundreds of transcripts with IGF2BP3-dependent changes in alternative splicing, including 97 differential splicing events in Lin- and 261 splicing events in

CD11b+ cells (Bayes factor ≥ 10, delta PSI ≥ 0.1, and minimum 20 reads supporting the event) (Supplemental Figure 6C). After merging all replicate eCLIP data for each cell type, we determined the position of eCLIP peaks relative to splice sites for splicing events identified by MISO (Figure 6B). Most event types, including skipped exons (SE), alternative first exons (AFE), alternative last exons (ALE), alternative 3' splice sites (A3SS), and alternative 5' splice sites (A5SS) exhibited both increases and decreases in percent spliced in (PSI), however, intron retention (RI) events showed a consistent reduction in splicing in the I3KO/MLL-Af4 cells (Figure 6C). A significant fraction of alternatively spliced transcripts contained IGF2BP3 binding sites in proximity of the splicing event ($P<2.2x10^{-16}$, Supplementary Figure 6D). Across all event types we found that the density of IGF2BP3 binding sites was strongest near the 3'splice site (3'ss), with additional signal near the 5' splice site (5'ss). This pattern was observed for each distinct splicing event class that MISO identified, with retained introns exhibiting the strongest bias towards the 3'ss (Supplemental Figure 6E). This positional bias in the data was noted for some differentially expressed genes, such as *Hoxa9*, *Hoxa7*, and *Cd69* (Figure 6D). *Hoxa9* is known to be alternatively spliced, with two well-characterized transcripts, full-length *Hoxa9* and truncated (homeobox-less) *Hoxa9T* (He et al., 2012; Stadler et al., 2014). We designed and validated RT-qPCR primers to measure the two RNA isoforms, finding that I3KO/MLL-Af4 cells showed an alteration in the ratio of the two isoforms (Figure 6F). This was in addition to our previous finding that the total transcript (using primers that are isoform-agnostic) was also downregulated in I3KO/MLL-Af4 cells (Figure 5E). Hence, the net effect of IGF2BP3 may be multi-pronged—there is a strong impact on steady state mRNA levels and potentially an impact on splicing. Taken together, these data demonstrate that IGF2BP3 functions in regulation of alternative pre-mRNA splicing in bulk leukemia cells and progenitor cells.

DISCUSSION

Here, we have generated an *Igf2bp3*–deficient murine model and queried MLL-Af4 mediated leukemogenesis. We demonstrated that *Igf2bp3* is required for the efficient initiation of leukemia and that this regulates the number and frequency of MLL-Af4 LICs. *Igf2bp3* regulates the expression of numerous critical transcripts in the *Hoxa* locus and the Ras signaling pathway, leading to dysregulated gene expression and enhanced downstream signaling, thereby promoting leukemogenesis.

MLL-AF4 driven leukemogenesis is associated with massive transcriptional dysregulation, mediated by the fusion of a histone methyltransferase with a factor involved in the super elongation complex (Smith et al., 2011). We confirm here that *Igf2bp3* is a direct transcriptional target of the MLL-AF4 fusion protein. Interestingly, IGF2BP3 itself seems to positively regulate MLL-AF4 transcriptional targets, based on our analysis provided here. Together, these data suggest that IGF2BP3 forms a novel post-transcriptional feed-forward loop that stabilizes and/or enhances the expression of MLL-Af4 transcriptional targets. Because of this unique relationship, and its relatively restricted pattern of expression in MLL-translocated leukemia, it is not clear if IGF2BP3 may play a role in other leukemia subtypes. However, it is worth noting that IGF2BP3 overexpression is noted in a wide range of cancer types and, hence, additional work is required to establish its role in other types of hematologic and non-hematologic malignancy.

In our previous study, we determined that IGF2BP3 is required for B-ALL cell survival, and that overexpression of IGF2BP3 in the bone marrow of mice leads to a pathologic expansion of hematopoietic stem and progenitor cells (Palanichamy et al., 2016). Here, using the MLL-Af4 leukemia model, we found that the deletion of *Igf2bp3* caused a striking delay in leukemia development and significantly increased the survival of MLL-Af4 mice. Furthermore, *Igf2bp3* deficiency greatly attenuated the aggressiveness of the disease. This was demonstrated by significant decreases in WBC counts, spleen weights, and infiltrating leukemic cells visualized in histopathological analysis of hematopoietic tissues. Although MLL-Af4 drives an acute myeloid

leukemia in mice (Lin et al., 2016), it is important to note that *MLL*r leukemias often show lineage infidelity and plasticity, leading to difficulties in applying targeted therapy (Rayes et al., 2016). While our prior work focused on IGF2BP3 in B-lineage *MLL*r leukemia, the current work suggests its broader applicability to all *MLL*r leukemia. Hence, IGF2BP3 may be a constant factor to target across the phenotypic range of *MLL*r leukemia and may be less subject to change in response to targeted therapy.

We also determined that *Igf2bp3* regulates the numbers and function of leukemia-initiating cells (LICs). Importantly, the effect of *Igf2bp3* deletion was restricted to LICs and did not significantly impact normal HSC function. Deletion of *Igf2bp3* led to a LIC disadvantage *in vivo* and *in vitro*, using both the I3KO mouse and a novel, orthogonal system utilizing CRISPR/Cas9-mediated deletion of *Igf2bp3*. LICs have been defined as cells that can self-renew and have the capability to produce downstream bulk leukemia cells (Magee et al., 2012). The persistence of these LICs is thought to contribute to relapse after treatment in several different leukemia subtypes (Bao et al., 2006; Chu et al., 2011; Diehn et al., 2009; Merlos-Suárez et al., 2011). In *MLL*r leukemia, LICs have been shown to have a high frequency in tumors and co-expression of mature lineage-restricted cell markers, with some excellent work in mouse models (Krivtsov et al., 2006; Somervaille and Cleary, 2006; Somervaille et al., 2009). However, the details of human LICs, particularly in MLL-AF4 leukemia, are less well known (Agraz-Doblas et al., 2019; Bardini et al., 2015; Barrett et al., 2016; Metzler et al., 2006). The role of IGF2BP3 in such cells will be of great interest and is a future direction for our work.

Previously, we discovered that IGF2BP3 interacts primarily with the 3'UTR of its target transcripts via iCLIP-seq (Palanichamy et al., 2016). In this study, we determined that IGF2BP3 targets many transcripts within intronic regions and near splice sites in addition to the 3'UTR, suggesting additional roles in post-transcriptional gene regulation. This difference may be due to the use of the eCLIP technique or the focused application on primary cells as opposed to cell lines. It is not entirely surprising, however, since RBPs are known to regulate gene expression at

several steps at the post-transcriptional level through mRNA operons (Keene, 2007; Keene and Lager, 2005). Furthermore, a recent study has shown that IGF2BP3 may regulate alternative splicing in the PKM gene in lung cancer cells (Xueqing et al., 2020). In line with this study, we found dynamic alternative splicing events that reflected various categories of alternative splicing phenomena, including retained Introns, alternative 5' and 3' splice sites, and skipped exons. In this light, it is interesting to note that intron retention has recently been reported to be a mechanism of transcriptome diversification in cancer and, specifically, in leukemia (Dvinge and Bradley, 2015; Wang et al., 2019). With this unexpected, novel discovery and our prior work detailing interactions with the 3'UTR, it is very likely that IGF2BP3 regulates specific mRNA operons through multiple post-transcriptional mechanisms in MLL-Af4 driven leukemia.

As an RBP, the function of IGF2BP3 is intimately connected to the underlying transcriptional program—IGF2BP3 can only act on transcripts that are specifically induced in the cell type where it is expressed. Hence, the finding of unique sets of genes that are bound and regulated by IGF2BP3 in Lin- and CD11b+ cells is not entirely unexpected, given that transcription changes as the leukemia initiating cells differentiate into the bulk leukemic cells. This is similar to what has been observed for miRNAs, which post-transcriptionally regulate distinct gene expression programs in distinct cell types (Lechman et al., 2016). The significant enrichment of IGF2BP3-bound mRNAs in the sets of differentially regulated and differentially spliced transcripts confirms a direct regulatory effect. However, further work is required to confirm functional relationships between the specific transcripts that are regulated and the phenotypic effects driven by IGF2BP3.

Notably, these differentially regulated transcripts showed significant enrichment for the KEGG transcriptional misregulation in cancer term as well as the GO oxidative phosphorylation term. Notable IGF2BP3 targets included critical transcripts in the *Hoxa* cluster such as *Hoxa9, Hoxa10, and Hoxa7.* HOXA9 is induced by MLL-AF4, plays a role in normal hematopoiesis, and is required for the survival of MLL-rearranged leukemia (Ernst et al., 2004b; Faber et al., 2009;

Imamura et al., 2002; Lawrence et al., 2005; Pineault et al., 2002; Rozovskaia et al., 2001). Furthermore, Hoxa9 is an alternatively spliced gene, with co-expression of a homeodomain-less splice variant, *Hoxa9T*, together with *Hoxa9*, shown to be necessary for full leukemogenic transformation (He et al., 2012; Stadler et al., 2014). Hence, *Igf2bp3* may act through upregulation of *Hoxa9* and *Hoxa9T* through multiple post-transcriptional mechanisms to promote MLL-Af4 driven leukemogenesis and impact the function of MLL-Af4 LICs. In addition, HOXA9 may play a role in the regulation of oxidative phosphorylation (Lynch et al., 2019), and it is tempting to speculate that the observed *Igf2bp3*-dependent impact on LICs is a consequence of dysregulated oxidative phosphorylation, a key pathway that regulates LICs. Importantly, because *Igf2bp3* was not required for steady-state hematopoiesis, in contrast to HOXA9, it may represent a more attractive target.

Work from our lab and others have demonstrated that IGF2BP3 targets a wide array of oncogenic transcripts and pathways, including CDK6 and MYC (Palanichamy et al., 2016). Here, we found that IGF2BP3 targets and modulates the expression of many transcripts within the Ras signaling pathway and its downstream effector pathways. RAS proteins control numerous cellular processes such as proliferation and survival, and are amongst the most commonly mutated genes in cancer (Downward, 2003; Schubbert et al., 2007). Interestingly, while *MLL*r leukemia has a paucity of additional mutations, the mutations that are present are in found mainly in the RAS signaling pathway (Agraz-Doblas et al., 2019; Andersson et al., 2015; Chandra et al., 2010; Emerenciano et al., 2015; Hyrenius-Wittsten et al., 2018; Kerstjens et al., 2017; Lavallée et al., 2015; Trentin et al., 2016). Moreover, several studies have shown selective activity against MLL-r leukemia cell lines and primary samples *in vitro* by MEK inhibitors, suggesting an important role for signaling downstream of RAS mutations in leukemia cell survival and proliferation (Kampen et al., 2014; Kerstjens et al., 2017; Lavallée et al., 2015).

Here, we determined that *Igf2bp3* is required for the efficient initiation of MLL-Af4 driven leukemia as well as for the development of and self-renewal capability of MLL-Af4 LICs.

Mechanistically, IGF2BP3 binds to hundreds of transcripts and modulates their expression *in vivo* and *in vitro* through multiple, complex post-transcriptional mechanisms. We describe a novel positional bias for IGF2BP3 binding in leukemic cells isolated from an *in vivo* model, a notable advance. In summary, our study demonstrated that IGF2BP3 is an amplifier of *MLL*r leukemogenesis by targeting *Hoxa* transcripts essential for leukemia-initiating cell function and targeting Ras signaling pathway transcripts, thereby controlling multiple critical downstream effector pathways required for disease initiation and severity. Our findings highlight IGF2BP3 as a necessary regulator of MLLr leukemia and a potential therapeutic target for this disease.

METHODS

ChIP-PCR. RS4;11 and SEM cells were used for ChIP assays as previously described (Janardhan et al., 2017). Primer sequences for the IGF2BP3 promoter region were provided by James Mulloy (University of Cincinnati College of Medicine)(Lin et al., 2016).

Western Blotting and RT-qPCR. Protein and mRNA extracts were prepared, and Western Blot/RT-qPCR performed as previously described (Fernando et al., 2017). Primers for qPCR and antibodies used for Western blotting are listed in Table S4.

Plasmids. The MSCV-MLL-flag-*Af4* plasmid was kindly provided by Michael Thirman (University of Chicago, Department of Medicine) through MTA (Lin et al., 2016). The non-targeting or *Igf2bp3* sgRNA was cloned into an in-house MSCV-hU6-sgRNA-EFS-mCherry vector.

Retroviral transduction and bone marrow transplantation. Retroviral transduction and bone marrow transplantation (BMT) were completed as previously described (Fernando et al., 2017; O'Connell et al., 2010; Rao et al., 2010). 5-FU enriched BM and Lin- cells were spin-infected four times with MSCV-MLL-flag-*Af4* virus at 30°C for 45 minutes in the presence of polybrene. Cells were selected with 400 µg/ml of G418 for 7 days. For sgRNA-mediated knockout, MLL-Af4 overexpressing Cas9-GFP cells were retrovirally infected with MSCV-hU6-NT/I3sgRNA-EFS-mCherry. The selected cells were then cultured for colony formation assays or injected into lethally irradiated mice.

Mice. C57BL/6J and B6J.129(Cg)-Gt(ROSA)26Sor$^{tm1.1(CAG\text{-}cas9*,\text{-}EGFP)Fezh}$/J (Cas9-GFP) mice were obtained from Jackson Laboratory. For *Igf2bp3* KO mouse generation, the UCI Transgenic Mouse Facility utilized CRISPR/Cas9 to insert loxP sites flanking exon 2 of *Igf2bp3* to generate *Igf2bp3*$^{f/f}$ mice. We originally attempted to generate conditional KO mice by breeding the *Igf2bp3*$^{f/f}$ mice

with Vav1-Cre mice. Consistent with prior reports, we found that this strategy led to “leaky” Cre expression, resulting in germline deletion (Croker et al., 2004; de Boer et al., 2003; Georgiades et al., 2002; Heffner et al., 2012; Joseph et al., 2013). To isolate the floxed and deletion (del) alleles, we back-crossed the mice onto C57BL/6 mice, successfully confirming germline, Mendelian transmission of the del and floxed alleles in two successive generations (Table S1). Mice heterozygous for the del allele were mated together, with the production of a homozygous deletion of *Igf2bp3*, resulting in the *Igf2bp3*$^{del/del}$ mice (I3KO) used in this study.

Cell culture. RS4;11, SEM, 70Z/3 and HEK 293T cell lines were cultured as previously described (Fernando et al., 2017). Lin- cells were cultured in IMDM with 15% fetal bovine serum supplemented with SCF, IL-6, FLT3, and TPO. CD11b+ cells were isolated from splenic tumors for positive selection by CD11b antibody and MACS (Miltenyi).

Flow cytometry. Blood, BM, thymus, and spleen were collected from the mice under sterile conditions at the indicated time points and staining performed as previously described (Contreras et al., 2015; Fernando et al., 2017). The list of antibodies used is provided in Table S4. Flow cytometry was performed on a BD FACS LSRII. Analysis was performed using FlowJo software.

Histopathology. Fixation and sectioning has been described previously (O'Connell et al., 2010). Analysis was performed by a board certified hematopathologist (D.S. Rao).

Competitive repopulation assay and secondary leukemia transplantation. Competitive repopulation experiments were completed as previously described (Palanichamy et al., 2016). For leukemia transplantation, BM was collected from WT/MLL-Af4 or I3KO/MLL-Af4 mice that succumbed to leukemia at 10-14 weeks post-transplantation and injected into 8-week-old immunocompetent CD45.1+ female mice.

eCLIP. IGF2BP3 crosslinking-immunoprecipitation studies were carried out from a minimum of two biological replicates with two technical replicates (four immunoprecipitations per cell type) and size matched input (smInput) samples in each cell type using Eclipse BioInnovations eCLIP kit. Briefly, $5x10^5$ cells were crosslinked with 245nm UV radiation at 400mJoules/cm^2. Crosslinked cell lysates were treated with RNAse I to fragment RNA and immunoprecipitated with anti-IGF2BP3 antibody (MBL RN009P) coupled to magnetic Protein G beads. Paired-end RNA sequencing was performed on the Illumina HiSeq4000 system at the UCSF Genomics Core Facility. Peaks were called using CLIPper (Lovci et al., 2013). Peaks were filtered based on appearance in the smInput (FS1). Annotation of the genomic location of the peaks and motif enrichment analysis were performed using HOMER (Heinz et al., 2010) annotatePeaks.pl and findMotifs.pl, respectively. Background for the peaks within differentially expressed genes was simulated using bedtools (Heinz et al., 2010; Quinlan and Hall, 2010) and shuffled 1000 times.

RNA seq. Single-end, strand-specific RNA sequencing was performed on the Illumina HiSeq3000 system for the Lin- and CD11b+ samples, resulting in 15-20 million reads per sample, at the UCLA Technology Center for Genomics & Bioinformatics. Our analysis pipeline has been previously described (Palanichamy et al., 2016). Enrichment analysis for KEGG pathways and Gene Ontology (GO) biological processes terms was completed with the Metascape analysis tool (http://metascape.org)(Zhou et al., 2019). Gene Set Enrichment Analysis (GSEA) was completed using the GSEAPreranked software on both the Lin- and CD11b+ DESeq datasets after calculation of π-value (Mootha et al., 2003; Subramanian et al., 2005; Xiao et al., 2014) to compare to the Hallmark and GO gene sets within the Molecular Signatures Database.

RNA seq data analysis. The RNA seq reads were mapped to the mouse genome assembly mm10 using STAR version X. Repeat sequences were masked using Bowtie 2 (Langmead and Salzberg, 2012) and RepeatMasker elements (Tarailo-Graovac and Chen, 2009). Differentially

expressed genes were identified using DESeq2 (Love et al., 2014) on the CD11b dataset and fdrtool (Strimmer, 2008a; Strimmer, 2008b) on the Lin- dataset. Multiple testing correction was done using the Benjamini-Hochberg method. Differentially expressed genes were considered significant if adjusted p-value < 0.1 and log2FC > 1. All data collection and parsing were completed with bash and python2.7. Statistical analyses were performed using R programming language version 3.5.1.

Estimation of alternative splicing. Mixture of Isoforms (MISO)1 Bayesian Inference model v0.5.4 was used to quantify alternative splicing events. The MISO event database for pairwise alternative splicing events for mm10 ("exon-centric annotation") was downloaded from hollywood.mit.edu/burgelab/miso/annotations/. After MISO quantified the percent spliced in (PSI) for each event by counting the number of reads supporting both events and the reads that are unique to each isoform, we calculated delta PSI by subtracting PSI from the WT with the I3KO sample for each alternative event. Finally, we filtered for significant and differential splicing events between wild-type and knockdown samples by requiring that delta PSI > 0.1, the Bayes factor ≥10, and the sum of exclusion and inclusion reads ≥ 10.

Statistics. Data represent mean ±SD for continuous numerical data, unless otherwise noted in the figure legends. One-way ANOVA followed by Bonferroni's multiple comparisons test or 2-tailed Student's t tests were performed using GraphPad Prism software. One-way ANOVA followed by Bonferroni's multiple comparisons test was performed in experiments with more than two groups.

Data Sharing Statement. Raw and analyzed data have been deposited onto the NCBI Gene Expression Omnibus (GEO) repository (GSE156115).

AUTHOR CONTRIBUTIONS

T.M.T., J.B., N.N., J.P., J.D., T.L., J.K.P., A.K.J., M.P., and J.K. performed experiments. T.M.T., J.P., and S.K. analyzed results and made the figures. O.S. provided experimental resource. T.M.T. and D.S.R. designed the research and wrote the paper. T.M.T., J.B., N.N., J.P., T.L., J.K.P., O.S., J.K., J.R.S., D.S.R. reviewed and edited the paper.

ACKNOWLEDGEMENTS

This work was supported by the Tumor Cell Biology Training Grant NIH T32 CA009056 (T.M.T.), NIH/NIGMS R35GM130361 (J.R.S.), NIH/NCI R01CA166540 (D.S.R.), NIH/NCI R21CA197441 (D.S.R.), American Society of Hematology Bridge Grant (D.S.R.), UCLA Jonsson Comprehensive Cancer Center Seed Grant (D.S.R.) and STOPCancer/Barbara and Gary Luboff Mitzvah Fund Seed Grant (D.S.R.). Flow cytometry was performed in the Eli and Edythe Broad Center of Regenerative Medicine and Stem Cell Research UCLA Flow Cytometry Core Resource and the UCLA JCCC/CFAR Flow Cytometry Core Facility that is supported by NIH AI-28697, P30CA016042, the JCCC, the UCLA AIDS Institute, and the David Geffen School of Medicine at UCLA. The authors acknowledge the support of the Chao Family Comprehensive Cancer Center Transgenic Mouse Facility (TMF) Shared Resource, supported by the National Cancer Institute of the National Institutes of Health under award number P30CA062203. The content is solely the responsibility of the authors and does not necessarily represent the official views of the National Institutes of Health. The authors would like to thank Jon Neumann (TMF), Michael O. Alberti, and Jorge Contreras for their expertise and helpful discussions.

REFERENCES

Agraz-Doblas, A., C. Bueno, R. Bashford-Rogers, A. Roy, P. Schneider, M. Bardini, P. Ballerini, G. Cazzaniga, T. Moreno, C. Revilla, M. Gut, M.G. Valsecchi, I. Roberts, R. Pieters, P. De Lorenzo, I. Varela, P. Menendez, and R.W. Stam. 2019. Unraveling the cellular origin and clinical prognostic markers of infant B-cell acute lymphoblastic leukemia using genome-wide analysis. *Haematologica* 104:1176-1188.

Andersson, A.K., J. Ma, J. Wang, X. Chen, A.L. Gedman, J. Dang, J. Nakitandwe, L. Holmfeldt, M. Parker, J. Easton, R. Huether, R. Kriwacki, M. Rusch, G. Wu, Y. Li, H. Mulder, S. Raimondi, S. Pounds, G. Kang, L. Shi, J. Becksfort, P. Gupta, D. Payne-Turner, B. Vadodaria, K. Boggs, D. Yergeau, J. Manne, G. Song, M. Edmonson, P. Nagahawatte, L. Wei, C. Cheng, D. Pei, R. Sutton, N.C. Venn, A. Chetcuti, A. Rush, D. Catchpoole, J. Heldrup, T. Fioretos, C. Lu, L. Ding, C.-H. Pui, S. Shurtleff, C.G. Mullighan, E.R. Mardis, R.K. Wilson, T.A. Gruber, J. Zhang, J.R. Downing, and P. St. Jude Children's Research Hospital–Washington University Pediatric Cancer Genome. 2015. The landscape of somatic mutations in infant MLL-rearranged acute lymphoblastic leukemias. *Nature Genetics* 47:330-337.

Bao, S., Q. Wu, R.E. McLendon, Y. Hao, Q. Shi, A.B. Hjelmeland, M.W. Dewhirst, D.D. Bigner, and J.N. Rich. 2006. Glioma stem cells promote radioresistance by preferential activation of the DNA damage response. *Nature* 444:756-760.

Bardini, M., P.S. Woll, L. Corral, S. Luc, L. Wittmann, Z. Ma, L. Lo Nigro, G. Basso, A. Biondi, G. Cazzaniga, and S.E.W. Jacobsen. 2015. Clonal variegation and dynamic competition of leukemia-initiating cells in infant acute lymphoblastic leukemia with MLL rearrangement. *Leukemia* 29:38-50.

Barrett, Neil A., C. Malouf, C. Kapeni, Wendi A. Bacon, G. Giotopoulos, Sten Eirik W. Jacobsen, Brian J. Huntly, and K. Ottersbach. 2016. Mll-AF4 Confers Enhanced Self-Renewal and Lymphoid Potential during a Restricted Window in Development. *Cell Reports* 16:1039-1054.

Brien, C.A., A. Kreso, and C.H.M. Jamieson. 2010. Cancer Stem Cells and Self-renewal. *Clinical Cancer Research* 16:3113.

Brundage, M.E., P. Tandon, D.W. Eaves, J.P. Williams, S.J. Miller, R.H. Hennigan, A. Jegga, T.P. Cripe, and N. Ratner. 2014. MAF mediates crosstalk between Ras-MAPK and mTOR signaling in NF1. *Oncogene* 33:5626-5636.

Bursen, A., K. Schwabe, B. Rüster, R. Henschler, M. Ruthardt, T. Dingermann, and R. Marschalek. 2010. The AF4·MLL fusion protein is capable of inducing ALL in mice without requirement of MLL·AF4. *Blood* 115:3570-3579.

Chandra, P., R. Luthra, Z. Zuo, H. Yao, F. Ravandi, N. Reddy, G. Garcia-Manero, H. Kantarjian, and D. Jones. 2010. Acute Myeloid Leukemia With t(9;11)(p21–22;q23): Common Properties of Dysregulated Ras Pathway Signaling and Genomic Progression Characterize De Novo and Therapy-Related Cases. *American Journal of Clinical Pathology* 133:686-693.

Chen, W., Q. Li, W.A. Hudson, A. Kumar, N. Kirchhof, and J.H. Kersey. 2006. A murine Mll-AF4 knock-in model results in lymphoid and myeloid deregulation and hematologic malignancy. *Blood* 108:669-677.

Chu, S., T. McDonald, A. Lin, S. Chakraborty, Q. Huang, D.S. Snyder, and R. Bhatia. 2011. Persistence of leukemia stem cells in chronic myelogenous leukemia patients in prolonged remission with imatinib treatment. *Blood* 118:5565-5572.

Contreras, J.R., J.K. Palanichamy, T.M. Tran, T.R. Fernando, N.I. Rodriguez-Malave, N. Goswami, V.A. Arboleda, D. Casero, and D.S. Rao. 2015. MicroRNA-146a modulates B-cell oncogenesis by regulating Egr1. *Oncotarget* 6:11023-11037.

Croker, B.A., D. Metcalf, L. Robb, W. Wei, S. Mifsud, L. DiRago, L.A. Cluse, K.D. Sutherland, L. Hartley, E. Williams, J.-G. Zhang, D.J. Hilton, N.A. Nicola, W.S. Alexander, and A.W. Roberts. 2004. SOCS3 Is a Critical Physiological Negative Regulator of G-CSF Signaling and Emergency Granulopoiesis. *Immunity* 20:153-165.

Dawson, M.A., R.K. Prinjha, A. Dittmann, G. Giotopoulos, M. Bantscheff, W.-I. Chan, S.C. Robson, C.-w. Chung, C. Hopf, M.M. Savitski, C. Huthmacher, E. Gudgin, D. Lugo, S. Beinke, T.D. Chapman, E.J. Roberts, P.E. Soden, K.R. Auger, O. Mirguet, K. Doehner, R. Delwel, A.K. Burnett, P. Jeffrey, G. Drewes, K. Lee, B.J.P. Huntly, and T. Kouzarides. 2011. Inhibition of BET recruitment to chromatin as an effective treatment for MLL-fusion leukaemia. *Nature* 478:529-533.

de Boer, J., A. Williams, G. Skavdis, N. Harker, M. Coles, M. Tolaini, T. Norton, K. Williams, K. Roderick, A.J. Potocnik, and D. Kioussis. 2003. Transgenic mice with hematopoietic and lymphoid specific expression of Cre. *European Journal of Immunology* 33:314-325.

Diehn, M., R.W. Cho, N.A. Lobo, T. Kalisky, M.J. Dorie, A.N. Kulp, D. Qian, J.S. Lam, L.E. Ailles, M. Wong, B. Joshua, M.J. Kaplan, I. Wapnir, F.M. Dirbas, G. Somlo, C. Garberoglio, B. Paz, J. Shen, S.K. Lau, S.R. Quake, J.M. Brown, I.L. Weissman, and M.F. Clarke. 2009. Association of reactive oxygen species levels and radioresistance in cancer stem cells. *Nature* 458:780-783.

Downward, J. 2003. Targeting RAS signalling pathways in cancer therapy. *Nature Reviews Cancer* 3:11-22.

Dvinge, H., and R.K. Bradley. 2015. Widespread intron retention diversifies most cancer transcriptomes. *Genome Med* 7:45.

Emerenciano, M., T.d.C. Barbosa, B. de Almeida Lopes, C. Meyer, R. Marschalek, and M.S. Pombo-de-Oliveira. 2015. Subclonality and prenatal origin of RAS mutations in KMT2A (MLL)-rearranged infant acute lymphoblastic leukaemia. *British Journal of Haematology* 170:268-271.

Ennajdaoui, H., Jonathan M. Howard, T. Sterne-Weiler, F. Jahanbani, Doyle J. Coyne, Philip J. Uren, M. Dargyte, S. Katzman, Jolene M. Draper, A. Wallace, O. Cazarez, Suzanne C. Burns, M. Qiao, L. Hinck, Andrew D. Smith, Masoud M. Toloue, Benjamin J. Blencowe, Luiz O.F. Penalva, and Jeremy R. Sanford. 2016. IGF2BP3 Modulates the Interaction of Invasion-Associated Transcripts with RISC. *Cell Reports* 15:1876-1883.

Ernst, P., J.K. Fisher, W. Avery, S. Wade, D. Foy, and S.J. Korsmeyer. 2004a. Definitive Hematopoiesis Requires the Mixed-Lineage Leukemia Gene. *Developmental Cell* 6:437-443.

Ernst, P., M. Mabon, A.J. Davidson, L.I. Zon, and S.J. Korsmeyer. 2004b. An Mll-Dependent Hox Program Drives Hematopoietic Progenitor Expansion. *Current Biology* 14:2063-2069.

Eychène, A., N. Rocques, and C. Pouponnot. 2008. A new MAFia in cancer. *Nature Reviews Cancer* 8:683-693.

Faber, J., A.V. Krivtsov, M.C. Stubbs, R. Wright, T.N. Davis, M. van den Heuvel-Eibrink, C.M. Zwaan, A.L. Kung, and S.A. Armstrong. 2009. HOXA9 is required for survival in human MLL-rearranged acute leukemias. *Blood* 113:2375-2385.

Fernando, T.R., J.R. Contreras, M. Zampini, N.I. Rodriguez-Malave, M.O. Alberti, J. Anguiano, T.M. Tran, J.K. Palanichamy, J. Gajeton, N.M. Ung, C.J. Aros, E.V. Waters, D. Casero, G. Basso, M. Pigazzi, and D.S. Rao. 2017. The lncRNA CASC15 regulates SOX4 expression in RUNX1-rearranged acute leukemia. *Mol Cancer* 16:126.

Georgiades, P., S. Ogilvy, H. Duval, D.R. Licence, D.S. Charnock‐Jones, S.K. Smith, and C.G. Print. 2002. vavCre Transgenic mice: A tool for mutagenesis in hematopoietic and endothelial lineages. *genesis* 34:251-256.

Haddox, C.L., A.A. Mangaonkar, D. Chen, M. Shi, R. He, J.L. Oliveira, M.R. Litzow, A. Al-Kali, W.J. Hogan, and M.A. Elliott. 2017. Blinatumomab-induced lineage switch of B-ALL with t(4:11)(q21;q23) KMT2A/AFF1 into an aggressive AML: pre- and post-switch phenotypic, cytogenetic and molecular analysis. *Blood Cancer Journal* 7:e607-e607.

Hardy, R.R., and K. Hayakawa. 2001. B Cell Development Pathways. *Annual Review of Immunology* 19:595-621.

He, M., P. Chen, S. Arnovitz, Y. Li, H. Huang, M.B. Neilly, M. Wei, J.D. Rowley, J. Chen, and Z. Li. 2012. Two isoforms of HOXA9 function differently but work synergistically in human MLL-rearranged leukemia. *Blood Cells Mol Dis* 49:102-106.

Heffner, C.S., C. Herbert Pratt, R.P. Babiuk, Y. Sharma, S.F. Rockwood, L.R. Donahue, J.T. Eppig, and S.A. Murray. 2012. Supporting conditional mouse mutagenesis with a comprehensive cre characterization resource. *Nature Communications* 3:1218.

Heinz, S., C. Benner, N. Spann, E. Bertolino, Y.C. Lin, P. Laslo, J.X. Cheng, C. Murre, H. Singh, and C.K. Glass. 2010. Simple combinations of lineage-determining transcription factors prime cis-regulatory elements required for macrophage and B cell identities. *Molecular cell* 38:576-589.

Hyrenius-Wittsten, A., M. Pilheden, H. Sturesson, J. Hansson, M.P. Walsh, G. Song, J.U. Kazi, J. Liu, R. Ramakrishan, C. Garcia-Ruiz, S. Nance, P. Gupta, J. Zhang, L. Rönnstrand, A. Hultquist, J.R. Downing, K. Lindkvist-Petersson, K. Paulsson, M. Järås, T.A. Gruber, J. Ma, and A.K. Hagström-Andersson. 2018. De novo activating mutations drive clonal evolution and enhance clonal fitness in KMT2A-rearranged leukemia. *Nature Communications* 9:1770.

Imamura, T., A. Morimoto, M. Takanashi, S. Hibi, T. Sugimoto, E. Ishii, and S. Imashuku. 2002. Frequent co-expression of HoxA9 and Meis1 genes in infant acute lymphoblastic leukaemia with MLL rearrangement. *British Journal of Haematology* 119:119-121.

Janardhan, H.P., Z.J. Milstone, M. Shin, N.D. Lawson, J.F. Keaney, Jr., and C.M. Trivedi. 2017. Hdac3 regulates lymphovenous and lymphatic valve formation. *The Journal of clinical investigation* 127:4193-4206.

Jønson, L., J. Christiansen, Thomas V.O. Hansen, J. Vikeså, Y. Yamamoto, and Finn C. Nielsen. 2014. IMP3 RNP Safe Houses Prevent miRNA-Directed HMGA2 mRNA Decay in Cancer and Development. *Cell Reports* 7:539-551.

Joseph, C., Julie M. Quach, Carl R. Walkley, Steven W. Lane, C. Lo Celso, and Louise E. Purton. 2013. Deciphering Hematopoietic Stem Cells in Their Niches: A Critical Appraisal of Genetic Models, Lineage Tracing, and Imaging Strategies. *Cell Stem Cell* 13:520-533.

Jude, C.D., L. Climer, D. Xu, E. Artinger, J.K. Fisher, and P. Ernst. 2007. Unique and Independent Roles for MLL in Adult Hematopoietic Stem Cells and Progenitors. *Cell Stem Cell* 1:324-337.

Kampen, K.R., A. ter Elst, H. Mahmud, F.J.G. Scherpen, S.H. Diks, M.P. Peppelenbosch, V. de Haas, V. Guryev, and E.S.J.M. de Bont. 2014. Insights in dynamic kinome reprogramming as a consequence of MEK inhibition in MLL-rearranged AML. *Leukemia* 28:589-599.

Katz, Y., E.T. Wang, E.M. Airoldi, and C.B. Burge. 2010. Analysis and design of RNA sequencing experiments for identifying isoform regulation. *Nature methods* 7:1009-1015.

Keene, J.D. 2007. RNA regulons: coordination of post-transcriptional events. *Nature Reviews Genetics* 8:533-543.

Keene, J.D., and P.J. Lager. 2005. Post-transcriptional operons and regulons co-ordinating gene expression. *Chromosome Research* 13:327-337.

Kerstjens, M., E.M.C. Driessen, M. Willekes, S.S. Pinhanços, P. Schneider, R. Pieters, and R.W. Stam. 2017. MEK inhibition is a promising therapeutic strategy for MLL-rearranged infant acute lymphoblastic leukemia patients carrying RAS mutations. *Oncotarget* 8:14835-14846.

Kobel, M., H. Xu, P.A. Bourne, B.O. Spaulding, M. Shih Ie, T.L. Mao, R.A. Soslow, C.A. Ewanowich, S.E. Kalloger, E. Mehl, C.H. Lee, D. Huntsman, and C.B. Gilks. 2009. IGF2BP3 (IMP3) expression is a marker of unfavorable prognosis in ovarian carcinoma of clear cell subtype. *Mod Pathol* 22:469-475.

Krivtsov, A.V., and S.A. Armstrong. 2007. MLL translocations, histone modifications and leukaemia stem-cell development. *Nature Reviews Cancer* 7:823-833.

Krivtsov, A.V., Z. Feng, M.E. Lemieux, J. Faber, S. Vempati, A.U. Sinha, X. Xia, J. Jesneck, A.P. Bracken, L.B. Silverman, J.L. Kutok, A.L. Kung, and S.A. Armstrong. 2008. H3K79 Methylation Profiles Define Murine and Human MLL-AF4 Leukemias. *Cancer Cell* 14:355-368.

Krivtsov, A.V., D. Twomey, Z. Feng, M.C. Stubbs, Y. Wang, J. Faber, J.E. Levine, J. Wang, W.C. Hahn, D.G. Gilliland, T.R. Golub, and S.A. Armstrong. 2006. Transformation from committed progenitor to leukaemia stem cell initiated by MLL–AF9. *Nature* 442:818-822.

Langmead, B., and S.L. Salzberg. 2012. Fast gapped-read alignment with Bowtie 2. *Nature Methods* 9:357-359.

Lavallée, V.-P., I. Baccelli, J. Krosl, B. Wilhelm, F. Barabé, P. Gendron, G. Boucher, S. Lemieux, A. Marinier, S. Meloche, J. Hébert, and G. Sauvageau. 2015. The

transcriptomic landscape and directed chemical interrogation of MLL-rearranged acute myeloid leukemias. *Nature Genetics* 47:1030-1037.

Lawrence, H.J., J. Christensen, S. Fong, Y.-L. Hu, I. Weissman, G. Sauvageau, R.K. Humphries, and C. Largman. 2005. Loss of expression of the Hoxa-9 homeobox gene impairs the proliferation and repopulating ability of hematopoietic stem cells. *Blood* 106:3988-3994.

Lechman, Eric R., B. Gentner, Stanley W.K. Ng, Erwin M. Schoof, P. van Galen, James A. Kennedy, S. Nucera, F. Ciceri, Kerstin B. Kaufmann, N. Takayama, Stephanie M. Dobson, A. Trotman-Grant, G. Krivdova, J. Elzinga, A. Mitchell, B. Nilsson, Karin G. Hermans, K. Eppert, R. Marke, R. Isserlin, V. Voisin, Gary D. Bader, Peter W. Zandstra, Todd R. Golub, Benjamin L. Ebert, J. Lu, M. Minden, Jean C.Y. Wang, L. Naldini, and John E. Dick. 2016. miR-126 Regulates Distinct Self-Renewal Outcomes in Normal and Malignant Hematopoietic Stem Cells. *Cancer Cell* 29:214-228.

Lewis, A., C.S. Park, M. Puppi, and H.D. Lacorazza. 2019. KLF4 Controls Leukemic Stem Cell Self-Renewal in MLL-AF9-Induced Acute Myeloid Leukemia. *Blood* 134:1231-1231.

Lin, C., E.R. Smith, H. Takahashi, K.C. Lai, S. Martin-Brown, L. Florens, M.P. Washburn, J.W. Conaway, R.C. Conaway, and A. Shilatifard. 2010. AFF4, a Component of the ELL/P-TEFb Elongation Complex and a Shared Subunit of MLL Chimeras, Can Link Transcription Elongation to Leukemia. *Molecular Cell* 37:429-437.

Lin, S., Roger T. Luo, A. Ptasinska, J. Kerry, Salam A. Assi, M. Wunderlich, T. Imamura, Joseph J. Kaberlein, A. Rayes, Mark J. Althoff, J. Anastasi, Maureen M. O'Brien, Amom R. Meetei, Thomas A. Milne, C. Bonifer, James C. Mulloy, and Michael J. Thirman. 2016. Instructive Role of MLL-Fusion Proteins Revealed by a Model of t(4;11) Pro-B Acute Lymphoblastic Leukemia. *Cancer Cell* 30:737-749.

Lin, S., R.T. Luo, M. Shrestha, M.J. Thirman, and J.C. Mulloy. 2017. The full transforming capacity of MLL-Af4 is interlinked with lymphoid lineage commitment. *Blood* 130:903-907.

Lochhead, P., Y. Imamura, T. Morikawa, A. Kuchiba, M. Yamauchi, X. Liao, Z.R. Qian, R. Nishihara, K. Wu, J.A. Meyerhardt, C.S. Fuchs, and S. Ogino. 2012. Insulin-like growth factor 2 messenger RNA binding protein 3 (IGF2BP3) is a marker of unfavourable prognosis in colorectal cancer. *Eur J Cancer* 48:3405-3413.

Lovci, M.T., D. Ghanem, H. Marr, J. Arnold, S. Gee, M. Parra, T.Y. Liang, T.J. Stark, L.T. Gehman, S. Hoon, K.B. Massirer, G.A. Pratt, D.L. Black, J.W. Gray, J.G. Conboy, and G.W. Yeo. 2013. Rbfox proteins regulate alternative mRNA splicing through evolutionarily conserved RNA bridges. *Nature structural & molecular biology* 20:1434-1442.

Love, M.I., W. Huber, and S. Anders. 2014. Moderated estimation of fold change and dispersion for RNA-seq data with DESeq2. *Genome Biology* 15:550.

Lynch, J.R., B. Salik, P. Connerty, B. Vick, H. Leung, A. Pijning, I. Jeremias, K. Spiekermann, T. Trahair, T. Liu, M. Haber, M.D. Norris, A.J. Woo, P. Hogg, J. Wang, and J.Y. Wang. 2019. JMJD1C-mediated metabolic dysregulation contributes to HOXA9-dependent leukemogenesis. *Leukemia* 33:1400-1410.

Magee, Jeffrey A., E. Piskounova, and Sean J. Morrison. 2012. Cancer Stem Cells: Impact, Heterogeneity, and Uncertainty. *Cancer Cell* 21:283-296.

Merlos-Suárez, A., Francisco M. Barriga, P. Jung, M. Iglesias, María V. Céspedes, D. Rossell, M. Sevillano, X. Hernando-Momblona, V. da Silva-Diz, P. Muñoz, H. Clevers, E. Sancho, R. Mangues, and E. Batlle. 2011. The Intestinal Stem Cell Signature Identifies Colorectal Cancer Stem Cells and Predicts Disease Relapse. *Cell Stem Cell* 8:511-524.

Metzler, M., A. Forster, R. Pannell, M.J. Arends, A. Daser, M.N. Lobato, and T.H. Rabbitts. 2006. A conditional model of MLL-AF4 B-cell tumourigenesis using invertor technology. *Oncogene* 25:3093-3103.

Meyer, C., T. Burmeister, D. Gröger, G. Tsaur, L. Fechina, A. Renneville, R. Sutton, N.C. Venn, M. Emerenciano, M.S. Pombo-de-Oliveira, C. Barbieri Blunck, B. Almeida Lopes, J. Zuna, J. Trka, P. Ballerini, H. Lapillonne, M. De Braekeleer, G. Cazzaniga, L. Corral Abascal, V.H.J. van der Velden, E. Delabesse, T.S. Park, S.H. Oh, M.L.M. Silva, T. Lund-Aho, V. Juvonen, A.S. Moore, O. Heidenreich, J. Vormoor, E. Zerkalenkova, Y. Olshanskaya, C. Bueno, P. Menendez, A. Teigler-Schlegel, U. zur Stadt, J. Lentes, G. Göhring, A. Kustanovich, O. Aleinikova, B.W. Schäfer, S. Kubetzko, H.O. Madsen, B. Gruhn, X. Duarte, P. Gameiro, E. Lippert, A. Bidet, J.M. Cayuela, E. Clappier, C.N. Alonso, C.M. Zwaan, M.M. van den Heuvel-Eibrink, S. Izraeli, L. Trakhtenbrot, P. Archer, J. Hancock, A. Möricke, J. Alten, M. Schrappe, M. Stanulla, S. Strehl, A. Attarbaschi, M. Dworzak, O.A. Haas, R. Panzer-Grümayer, L. Sedék, T. Szczepański, A. Caye, L. Suarez, H. Cavé, and R. Marschalek. 2018. The MLL recombinome of acute leukemias in 2017. *Leukemia* 32:273-284.

Milne, T.A., J. Kim, G.G. Wang, S.C. Stadler, V. Basrur, S.J. Whitcomb, Z. Wang, A.J. Ruthenburg, K.S.J. Elenitoba-Johnson, R.G. Roeder, and C.D. Allis. 2010. Multiple Interactions Recruit MLL1 and MLL1 Fusion Proteins to the HOXA9 Locus in Leukemogenesis. *Molecular Cell* 38:853-863.

Mohan, M., C. Lin, E. Guest, and A. Shilatifard. 2010. Licensed to elongate: a molecular mechanism for MLL-based leukaemogenesis. *Nature Reviews Cancer* 10:721-728.

Montes, R., V. Ayllon, I. Gutierrez-Aranda, I. Prat, M.C. Hernandez-Lamas, L. Ponce, S. Bresolin, G. te Kronnie, M. Greaves, C. Bueno, and P. Menendez. 2011. Enforced expression of MLL-AF4 fusion in cord blood CD34+ cells enhances the hematopoietic repopulating cell function and clonogenic potential but is not sufficient to initiate leukemia. *Blood* 117:4746-4758.

Moorman, A.V., H.M. Ensor, S.M. Richards, L. Chilton, C. Schwab, S.E. Kinsey, A. Vora, C.D. Mitchell, and C.J. Harrison. 2010. Prognostic effect of chromosomal abnormalities in childhood B-cell precursor acute lymphoblastic leukaemia: results from the UK Medical Research Council ALL97/99 randomised trial. *The Lancet Oncology* 11:429-438.

Mootha, V.K., C.M. Lindgren, K.-F. Eriksson, A. Subramanian, S. Sihag, J. Lehar, P. Puigserver, E. Carlsson, M. Ridderstråle, E. Laurila, N. Houstis, M.J. Daly, N. Patterson, J.P. Mesirov, T.R. Golub, P. Tamayo, B. Spiegelman, E.S. Lander, J.N. Hirschhorn, D. Altshuler, and L.C. Groop. 2003. PGC-1α-responsive genes

involved in oxidative phosphorylation are coordinately downregulated in human diabetes. *Nature Genetics* 34:267-273.
Mueller, F., M. Bommer, U. Lacher, C. Ruhland, V. Stagge, G. Adler, T.M. Gress, and T. Seufferlein. 2003. KOC is a novel molecular indicator of malignancy. *British journal of cancer* 88:699-701.
Mueller-Pillasch, F., B. Pohl, M. Wilda, U. Lacher, M. Beil, C. Wallrapp, H. Hameister, W. Knochel, G. Adler, and T.M. Gress. 1999. Expression of the highly conserved RNA binding protein KOC in embryogenesis. *Mech Dev* 88:95-99.
Nguyen, Liem H., Daisy A. Robinton, Marc T. Seligson, L. Wu, L. Li, D. Rakheja, Sarah A. Comerford, S. Ramezani, X. Sun, Monisha S. Parikh, Erin H. Yang, John T. Powers, G. Shinoda, Samar P. Shah, Robert E. Hammer, George Q. Daley, and H. Zhu. 2014. Lin28b Is Sufficient to Drive Liver Cancer and Necessary for Its Maintenance in Murine Models. *Cancer Cell* 26:248-261.
O'Connell, R.M., A.B. Balazs, D.S. Rao, C. Kivork, L. Yang, and D. Baltimore. 2010. Lentiviral Vector Delivery of Human Interleukin-7 (hIL-7) to Human Immune System (HIS) Mice Expands T Lymphocyte Populations. *PLOS ONE* 5:e12009.
Palanichamy, J.K., T.M. Tran, J.M. Howard, J.R. Contreras, T.R. Fernando, T. Sterne-Weiler, S. Katzman, M. Toloue, W. Yan, G. Basso, M. Pigazzi, J.R. Sanford, and D.S. Rao. 2016. RNA-binding protein IGF2BP3 targeting of oncogenic transcripts promotes hematopoietic progenitor proliferation. *J Clin Invest* 126:1495-1511.
Park, S.-M., M. Gönen, L. Vu, G. Minuesa, P. Tivnan, T.S. Barlowe, J. Taggart, Y. Lu, R.P. Deering, N. Hacohen, M.E. Figueroa, E. Paietta, H.F. Fernandez, M.S. Tallman, A. Melnick, R. Levine, C. Leslie, C.J. Lengner, and M.G. Kharas. 2015. Musashi2 sustains the mixed-lineage leukemia–driven stem cell regulatory program. *The Journal of clinical investigation* 125:1286-1298.
Pineault, N., C.D. Helgason, H.J. Lawrence, and R.K. Humphries. 2002. Differential expression of Hox, Meis1, and Pbx1 genes in primitive cells throughout murine hematopoietic ontogeny. *Experimental Hematology* 30:49-57.
Pui, C.-H., W.L. Carroll, S. Meshinchi, and R.J. Arceci. 2011. Biology, Risk Stratification, and Therapy of Pediatric Acute Leukemias: An Update. *Journal of Clinical Oncology* 29:551-565.
Quinlan, A.R., and I.M. Hall. 2010. BEDTools: a flexible suite of utilities for comparing genomic features. *Bioinformatics (Oxford, England)* 26:841-842.
Rao, D.S., R.M. O'Connell, A.A. Chaudhuri, Y. Garcia-Flores, T.L. Geiger, and D. Baltimore. 2010. MicroRNA-34a Perturbs B Lymphocyte Development by Repressing the Forkhead Box Transcription Factor Foxp1. *Immunity* 33:48-59.
Rayes, A., R.L. McMasters, and M.M. O'Brien. 2016. Lineage Switch in MLL-Rearranged Infant Leukemia Following CD19-Directed Therapy. *Pediatr Blood Cancer* 63:1113-1115.
Riverso, M., V. Montagnani, and B. Stecca. 2017. KLF4 is regulated by RAS/RAF/MEK/ERK signaling through E2F1 and promotes melanoma cell growth. *Oncogene* 36:3322-3333.
Rozovskaia, T., E. Feinstein, O. Mor, R. Foa, J. Blechman, T. Nakamura, C.M. Croce, G. Cimino, and E. Canaani. 2001. Upregulation of Meis1 and HoxA9 in acute lymphocytic leukemias with the t(4 : 11) abnormality. *Oncogene* 20:874-878.

Schaeffer, D.F., D.R. Owen, H.J. Lim, A.K. Buczkowski, S.W. Chung, C.H. Scudamore, D.G. Huntsman, S.S. Ng, and D.A. Owen. 2010. Insulin-like growth factor 2 mRNA binding protein 3 (IGF2BP3) overexpression in pancreatic ductal adenocarcinoma correlates with poor survival. *BMC Cancer* 10:59.

Schneider, T., L.-H. Hung, M. Aziz, A. Wilmen, S. Thaum, J. Wagner, R. Janowski, S. Müller, S. Schreiner, P. Friedhoff, S. Hüttelmaier, D. Niessing, M. Sattler, A. Schlundt, and A. Bindereif. 2019. Combinatorial recognition of clustered RNA elements by the multidomain RNA-binding protein IMP3. *Nature Communications* 10:2266.

Schubbert, S., K. Shannon, and G. Bollag. 2007. Hyperactive Ras in developmental disorders and cancer. *Nature Reviews Cancer* 7:295-308.

Smith, E., C. Lin, and A. Shilatifard. 2011. The super elongation complex (SEC) and MLL in development and disease. *Genes & Development* 25:661-672.

Somervaille, T.C.P., and M.L. Cleary. 2006. Identification and characterization of leukemia stem cells in murine MLL-AF9 acute myeloid leukemia. *Cancer Cell* 10:257-268.

Somervaille, T.C.P., C.J. Matheny, G.J. Spencer, M. Iwasaki, J.L. Rinn, D.M. Witten, H.Y. Chang, S.A. Shurtleff, J.R. Downing, and M.L. Cleary. 2009. Hierarchical maintenance of MLL myeloid leukemia stem cells employs a transcriptional program shared with embryonic rather than adult stem cells. *Cell stem cell* 4:129-140.

Stadler, C.R., N. Vegi, M.A. Mulaw, K.E. Edmaier, V.P.S. Rawat, A. Dolnik, L. Bullinger, B. Heilmeier, L. Quintanilla-Fend, K. Spiekermann, W. Hiddemann, K. Döhner, H. Döhner, M. Feuring-Buske, and C. Buske. 2014. The leukemogenicity of Hoxa9 depends on alternative splicing. *Leukemia* 28:1838-1843.

Stoskus, M., E. Gineikiene, V. Valceckiene, B. Valatkaite, R. Pileckyte, and L. Griskevicius. 2011. Identification of characteristic IGF2BP expression patterns in distinct B-ALL entities. *Blood Cells, Molecules, and Diseases* 46:321-326.

Strimmer, K. 2008a. fdrtool: a versatile R package for estimating local and tail area-based false discovery rates. *Bioinformatics* 24:1461-1462.

Strimmer, K. 2008b. A unified approach to false discovery rate estimation. *BMC Bioinformatics* 9:303.

Subramanian, A., P. Tamayo, V.K. Mootha, S. Mukherjee, B.L. Ebert, M.A. Gillette, A. Paulovich, S.L. Pomeroy, T.R. Golub, E.S. Lander, and J.P. Mesirov. 2005. Gene set enrichment analysis: A knowledge-based approach for interpreting genome-wide expression profiles. *Proceedings of the National Academy of Sciences* 102:15545.

Takata, M., Y. Goto, N. Ichii, M. Yamaura, H. Murata, H. Koga, A. Fujimoto, and T. Saida. 2005. Constitutive Activation of the Mitogen-Activated Protein Kinase Signaling Pathway in Acral Melanomas. *Journal of Investigative Dermatology* 125:318-322.

Tamai, H., K. Miyake, M. Takatori, N. Miyake, H. Yamaguchi, K. Dan, T. Shimada, and K. Inokuchi. 2011. Activated K-Ras protein accelerates human MLL/AF4-induced leukemo-lymphomogenicity in a transgenic mouse model. *Leukemia* 25:888-891.

Tarailo-Graovac, M., and N. Chen. 2009. Using RepeatMasker to Identify Repetitive Elements in Genomic Sequences. *Current Protocols in Bioinformatics* 25:4.10.11-14.10.14.

Trentin, L., S. Bresolin, E. Giarin, M. Bardini, V. Serafin, B. Accordi, F. Fais, C. Tenca, P. De Lorenzo, M.G. Valsecchi, G. Cazzaniga, G.T. Kronnie, and G. Basso. 2016. Deciphering KRAS and NRAS mutated clone dynamics in MLL-AF4 paediatric leukaemia by ultra deep sequencing analysis. *Scientific reports* 6:34449-34449.

Wagle, M.-C., D. Kirouac, C. Klijn, B. Liu, S. Mahajan, M. Junttila, J. Moffat, M. Merchant, L. Huw, M. Wongchenko, K. Okrah, S. Srinivasan, Z. Mounir, T. Sumiyoshi, P.M. Haverty, R.L. Yauch, Y. Yan, O. Kabbarah, G. Hampton, L. Amler, S. Ramanujan, M.R. Lackner, and S.-M.A. Huang. 2018. A transcriptional MAPK Pathway Activity Score (MPAS) is a clinically relevant biomarker in multiple cancer types. *npj Precision Oncology* 2:7.

Wang, E., S.X. Lu, A. Pastore, X. Chen, J. Imig, S. Chun-Wei Lee, K. Hockemeyer, Y.E. Ghebrechristos, A. Yoshimi, D. Inoue, M. Ki, H. Cho, L. Bitner, A. Kloetgen, K.T. Lin, T. Uehara, T. Owa, R. Tibes, A.R. Krainer, O. Abdel-Wahab, and I. Aifantis. 2019. Targeting an RNA-Binding Protein Network in Acute Myeloid Leukemia. *Cancer Cell* 35:369-384.e367.

Wei, J., M. Wunderlich, C. Fox, S. Alvarez, J.C. Cigudosa, J.S. Wilhelm, Y. Zheng, J.A. Cancelas, Y. Gu, M. Jansen, J.F. DiMartino, and J.C. Mulloy. 2008. Microenvironment Determines Lineage Fate in a Human Model of MLL-AF9 Leukemia. *Cancer Cell* 13:483-495.

Wilkinson, Adam C., E. Ballabio, H. Geng, P. North, M. Tapia, J. Kerry, D. Biswas, Robert G. Roeder, C.D. Allis, A. Melnick, Marella F.T.R. de Bruijn, and Thomas A. Milne. 2013. RUNX1 Is a Key Target in t(4;11) Leukemias that Contributes to Gene Activation through an AF4-MLL Complex Interaction. *Cell Reports* 3:116-127.

Wu, Y., X. Tan, P. Liu, Y. Yang, Y. Huang, X. Liu, X. Meng, B. Yu, M. Wu, and H. Jin. 2019. ITGA6 and RPSA synergistically promote pancreatic cancer invasion and metastasis via PI3K and MAPK signaling pathways. *Experimental Cell Research* 379:30-47.

Xiao, Y., T.-H. Hsiao, U. Suresh, H.-I.H. Chen, X. Wu, S.E. Wolf, and Y. Chen. 2014. A novel significance score for gene selection and ranking. *Bioinformatics (Oxford, England)* 30:801-807.

Xueqing, H., Z. Jun, J. Yueqiang, L. Xin, H. Liya, F. Yuanyuan, Z. Yuting, Z. Hao, W. Hua, L. Jian, and Y. Tiejun. 2020. IGF2BP3 May Contributes to Lung Tumorigenesis by Regulating the Alternative Splicing of PKM. *Frontiers in Bioengineering and Biotechnology* 8:679.

Zhou, Y., B. Zhou, L. Pache, M. Chang, A.H. Khodabakhshi, O. Tanaseichuk, C. Benner, and S.K. Chanda. 2019. Metascape provides a biologist-oriented resource for the analysis of systems-level datasets. *Nature Communications* 10:1523.

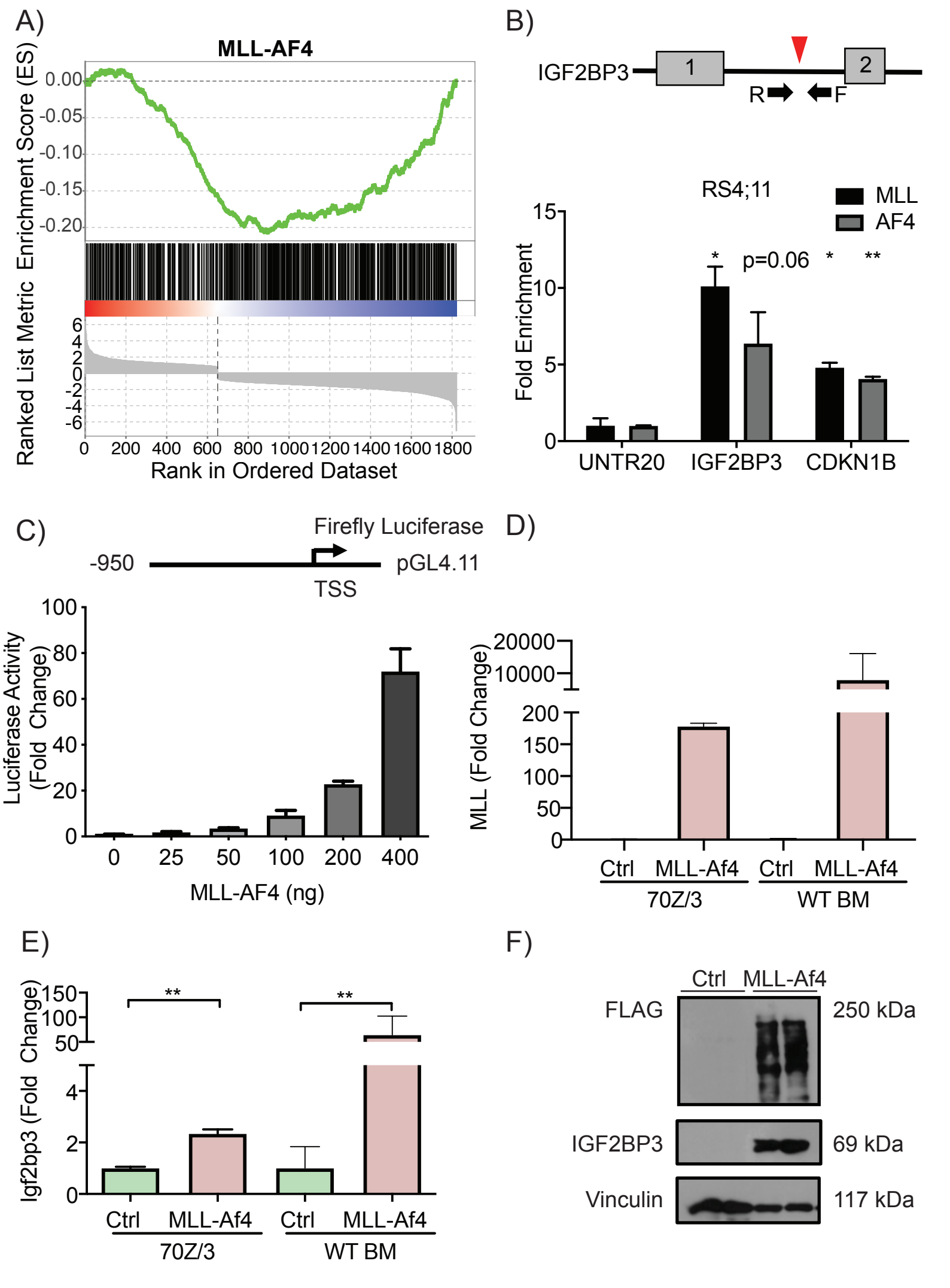
A)
MLL-AF4
Enrichment Score (ES)
0.00
-0.05
-0.10
-0.15
-0.20
Ranked List Metric
6
4
2
0
-2
-4
-6
0 200 400 600 800 1000 1200 1400 1600 1800
Rank in Ordered Dataset
B)
IGF2BP3
1
2
R
F
RS4;11
MLL
AF4
Fold Enrichment
15
10
5
0
*
p=0.06
*
**
UNTR20
IGF2BP3
CDKN1B
C)
Firefly Luciferase
-950
pGL4.11
TSS
Luciferase Activity (Fold Change)
100
80
60
40
20
0
0 25 50 100 200 400
MLL-AF4 (ng)
D)
MLL (Fold Change)
20000
10000
200
150
100
50
0
Ctrl MLL-Af4 Ctrl MLL-Af4
70Z/3
WT BM
E)
Igf2bp3 (Fold Change)
150
100
50
4
2
0
**
**
Ctrl MLL-Af4 Ctrl MLL-Af4
70Z/3
WT BM
F)
Ctrl MLL-Af4
FLAG
250 kDa
IGF2BP3
69 kDa
Vinculin
117 kDa

Figure 1

Figure 1: MLL-AF4 transcriptionally induces IGF2BP3.
A) GSEA of differentially expressed genes from IGF2BP3 depleted RS4;11 cells shows significant negative enrichment with MLL-AF4 ChIP targets (nominal P value: 0.001, FDR: 0.001, Normalized ES: -1.54)).
B) Schematic of MLL-AF4 binding site in intron 1 of IGF2BP3 (top). ChIP-qPCR shows fold enrichment for IGF2BP3 and CDKN1B with MLL and AF4 IP in RS4;11. Normalized to UNTR20, an untranscribed region (t-test; *P < 0.05, **P < 0.01).
C) Luciferase assay of the IGF2BP3 promoter shows a dose-dependent response to MLL-AF4.
D) Expression of MLL through RT-qPCR of 70Z/3 transduced with either control (Ctrl) or MLL-Af4 vector selected with G418 and MLL expression at the RNA level in the BM of WT recipients transplanted with Ctrl or MLL-Af4 HSPCs.
E) Induction of Igf2bp3 at the RNA level in selected 70Z/3 with MLL-Af4 and in the BM of WT recipients transplanted with Ctrl or MLL-Af4 HSPCs (bottom) (t-test; **P < 0.01) .
F) Induction of Igf2bp3 at the protein level in BM from mice transplanted with MLL-Af4 transduced WT donor HSPCs.

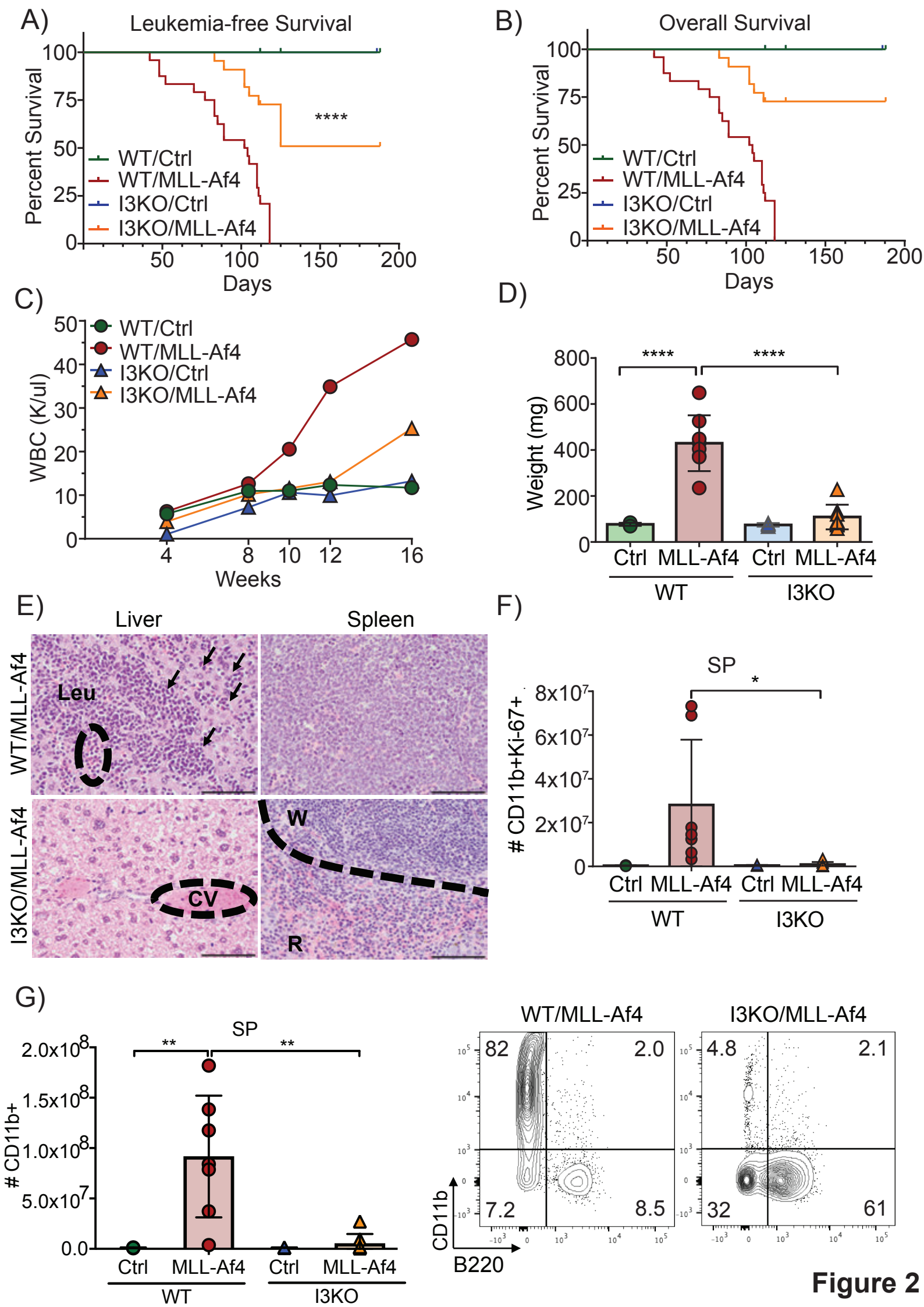
A)
Leukemia-free Survival
Percent Survival
Days
WT/Ctrl
WT/MLL-Af4
I3KO/Ctrl
I3KO/MLL-Af4
****
B)
Overall Survival
Percent Survival
Days
C)
WBC (K/ul)
Weeks
D)
Weight (mg)
Ctrl
MLL-Af4
WT
I3KO
E)
Liver
Spleen
WT/MLL-Af4
I3KO/MLL-Af4
Leu
CV
W
R
F)
SP
CD11b+Ki-67+
G)
SP
CD11b+
WT/MLL-Af4
I3KO/MLL-Af4
CD11b
B220
82
2.0
7.2
8.5
4.8
2.1
32
61

Figure 2

Figure 2: *Igf2bp3* deletion delays leukemogenesis and reduces disease severity.
A) Leukemia-free survival of mice transplanted with control (Ctrl) or MLL-Af4 transduced HSPCs from WT or Igf2bp3 KO mice (Kaplan-Meier method with Log-rank test; ****P < 0.0001).
B) Overall survival of mice transplanted with Ctrl or MLL-Af4 transduced HSPCs from WT or I3KO mice (n=12 WT/Ctrl, n=24 WT/MLL-Af4, n=7 I3KO/Ctrl, n=22 I3KO/MLL-Af4; Kaplan-Meier method with Log-rank test; ****P < 0.0001).
C) Time course of WBC in the PB of mice transplanted with Ctrl or MLL-Af4 transduced HSPCs from WT or I3KO mice (Data represented as means of three experiments; n=4 Ctrl, n=8 MLL-Af4 per experiment).
D) Spleen weights of mice transplanted with Ctrl or MLL-Af4 transduced HSPCs from WT or I3KO mice at 14 weeks (n= 4 Ctrl, n=8 MLL-Af4; one-way ANOVA followed by Bonferroni's multiple comparisons test; ****P < 0.0001).
E) H&E staining of liver and spleen of mice transplanted with mice transplanted with MLL-Af4 transduced HSPCs from WT or I3KO mice at 14 weeks. Scale bar:100 microns; CV=Central vein; W=White pulp; R=Red pulp; Leu= Leukemia; arrows showing infiltration.
F) Quantitation of CD11b+Ki67+ cells in the spleen at 14 weeks post-transplantation (n= 4 Ctrl, n=8 MLL-Af4; one-way ANOVA followed by Bonferroni's multiple comparisons test; *P < 0.05).
G) (Left) Number of CD11b+ in the SP of recipient mice that received Ctrl or MLL-Af4 transduced HSPCs from WT or I3KO mice at 14 weeks (one-way ANOVA followed by Bonferroni's multiple comparisons test; **P < 0.01). (Right) Corresponding representative FACS plots showing CD11b+ and B220+ cells in the SP.

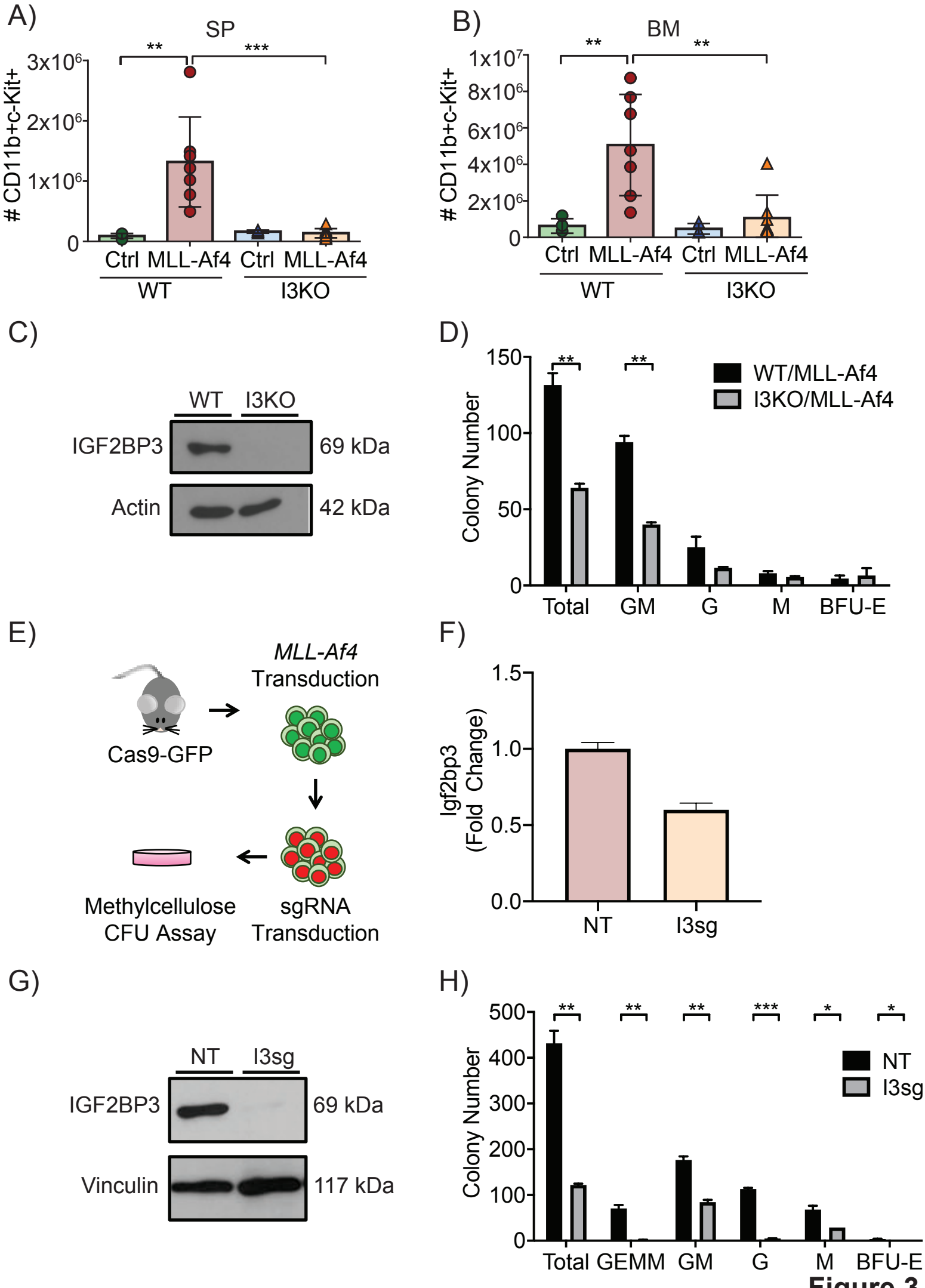
A)
SP
CD11b+c-Kit+
3x10⁶
2x10⁶
1x10⁶
0
**
***
Ctrl
MLL-Af4
Ctrl
MLL-Af4
WT
I3KO
B)
BM
CD11b+c-Kit+
1x10⁷
8x10⁶
6x10⁶
4x10⁶
2x10⁶
0
**
**
Ctrl
MLL-Af4
Ctrl
MLL-Af4
WT
I3KO
C)
WT
I3KO
IGF2BP3
69 kDa
Actin
42 kDa
D)
Colony Number
150
100
50
0
**
**
WT/MLL-Af4
I3KO/MLL-Af4
Total
GM
G
M
BFU-E
E)
MLL-Af4
Transduction
Cas9-GFP
Methylcellulose
CFU Assay
sgRNA
Transduction
F)
Igf2bp3
(Fold Change)
1.5
1.0
0.5
0.0
NT
I3sg
G)
NT
I3sg
IGF2BP3
69 kDa
Vinculin
117 kDa
H)
Colony Number
500
400
300
200
100
0
**
**
**
***
*
*
NT
I3sg
Total
GEMM
GM
G
M
BFU-E

Figure 3

Figure 3: *Igf2bp3* is required for LIC function in endpoint colony formation assays.

A) Quantification of CD11b+c-Kit+ cells in the spleen of recipient mice at 14 weeks post-transplantation (n= 4 Ctrl, n=8 MLL-Af4; one-way ANOVA followed by Bonferroni's multiple comparisons test; **P < 0.01).

B) Quantitation of CD11b+c-Kit+ cells in the BM 14 weeks post-transplantation (n= 4 Ctrl, n=8 MLL-Af4; one-way ANOVA followed by Bonferroni's multiple comparisons test; **P < 0.01, ***P < 0.001).

C) Expression of IGF2BP3 of in WT/MLL-Af4 and I3KO/MLL-Af4 immortalized Lin- cells at the protein level.

D) Colony formation assay of WT/MLL-Af4 and I3KO/MLL-Af4 immortalized Lin- cells (t-test; **P < 0.01).

E) Schematic of collection of Cas9-GFP MLL-Af4 Lin- cells and CRISPR-Cas9 mediated deletion of *Igf2bp3*.

F) Expression of Igf2bp3 in Cas9-GFP MLL-Af4 Lin- cells in non-targeting (NT) and Igf2bp3 deleted (I3sg) cells by RT-qPCR.

G) Expression of IGF2BP3 in NT and I3sg Cas9-GFP MLL-Af4 Lin- cells at the protein level.

H) Colony formation assay of NT and I3sg deleted Cas9-GFP MLL-Af4 Lin- cells (t-test; *P < 0.05, **P < 0.01, ***P <0.001).

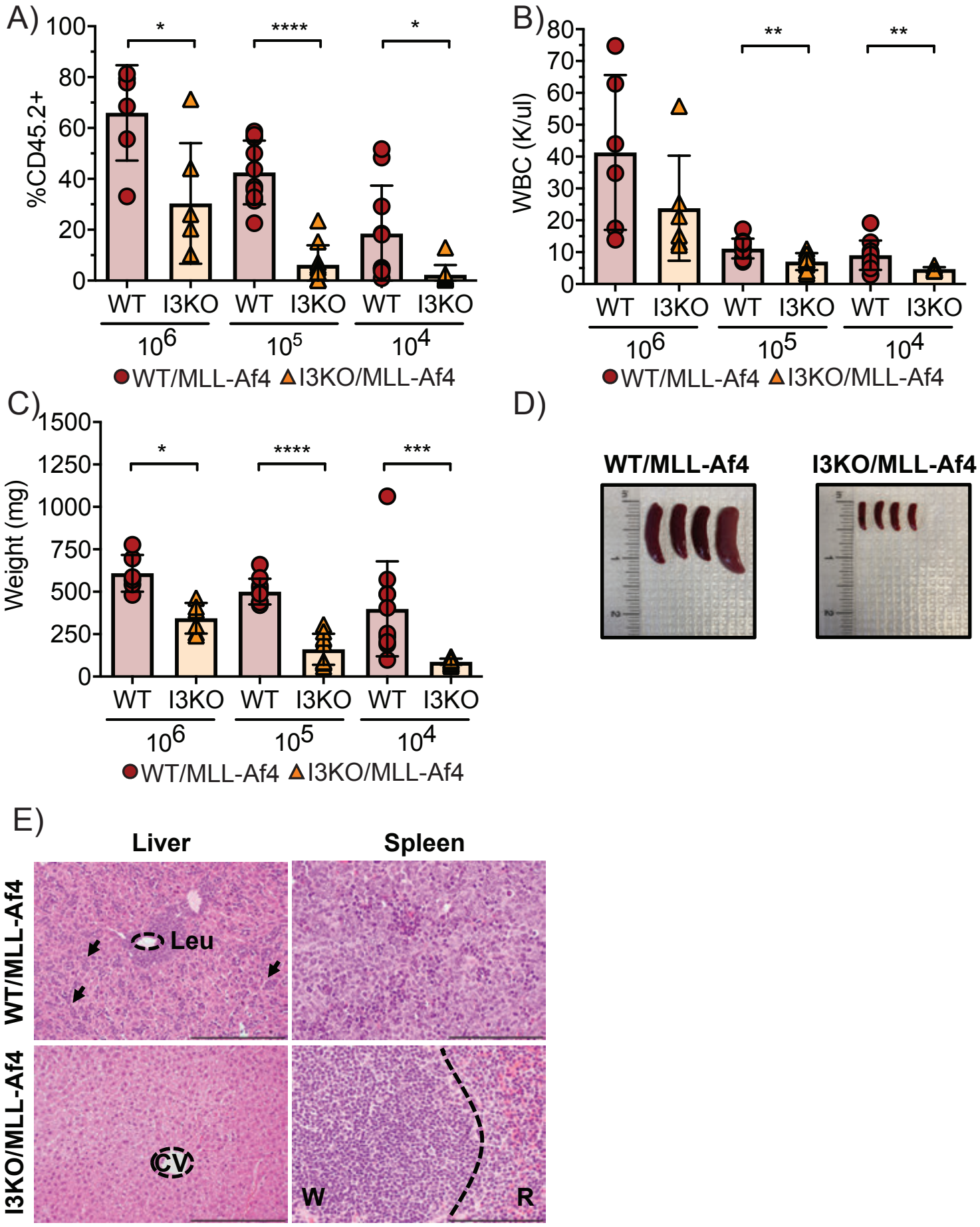
A)
%CD45.2+
100
80
60
40
20
0
*
****
*
WT
I3KO
WT
I3KO
WT
I3KO
10^6
10^5
10^4
WT/MLL-Af4
I3KO/MLL-Af4
B)
WBC (K/ul)
80
70
60
50
40
30
20
10
0
**
**
WT
I3KO
WT
I3KO
WT
I3KO
10^6
10^5
10^4
WT/MLL-Af4
I3KO/MLL-Af4
C)
Weight (mg)
1500
1250
1000
750
500
250
0
*
****
***
WT
I3KO
WT
I3KO
WT
I3KO
10^6
10^5
10^4
WT/MLL-Af4
I3KO/MLL-Af4
D)
WT/MLL-Af4
I3KO/MLL-Af4
E)
Liver
Spleen
WT/MLL-Af4
I3KO/MLL-Af4
Leu
CV
W
R

Figure 4

Figure 4: *Igf2bp3* deletion is necessary for MLL-Af4 leukemia-initiating cells to reconstitute mice *in vivo*.

A) Percentage of CD45.2+ in the peripheral blood of secondary transplanted mice from leukemic WT/MLL-Af4 or I3KO/MLL-Af4 donor mice at 10^6, 10^5, and 10^4 BM cells at 4 weeks post-transplantation (n= 6 10^6, n=10 10^5, n=10 10^4; t-test; *P < 0.05, ***P < 0.001, ****P < 0.0001).

B) WBC from PB of secondary transplanted mice from WT/MLL-Af4 or I3KO/MLL-Af4 BM 3-4 weeks post-transplant (n= 6 10^6, n=10 10^5, n=10 10^4; t-test; **P < 0.01).

C) Splenic weights of secondary transplanted mice at 4-5 weeks (n= 6 10^6, n=10 10^5, n=10 10^4; t-test; *P < 0.05, ***P < 0.001, ****P < 0.0001).

D) Images of splenic tumors in secondary mice transplanted with 10,000 BM cells from WT/MLL-Af4 mice (left) or I3KO/MLL-Af4 mice (right) at 5 weeks.

E) H&E staining of liver and spleen of secondary transplant recipients that received 10^5 cells at 4 weeks. Scale bar: liver, 200 microns; spleen, 100 microns; CV=Central vein; W=White pulp; R=Red pulp; Leu= Leukemia; arrows showing infiltration.

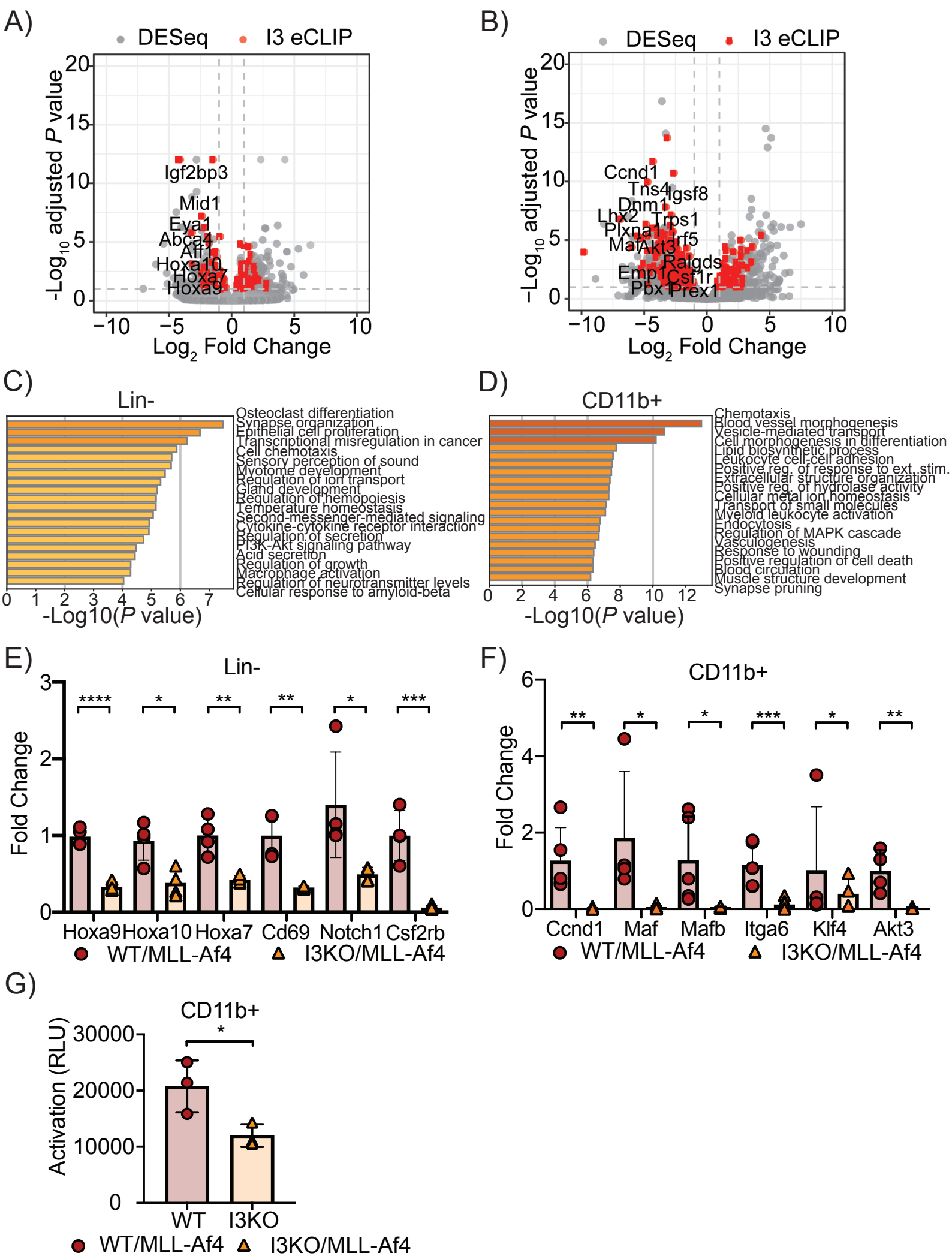
A)
DESeq
I3 eCLIP
-Log10 adjusted P value
Log2 Fold Change
Igf2bp3
Mid1
Eya1
Abca4
Aff1
Hoxa10
Hoxa7
Hoxa9
B)
DESeq
I3 eCLIP
-Log10 adjusted P value
Log2 Fold Change
Ccnd1
Tns4
Igsf8
Dnm1
Lhx2
Trps1
Plxna1
Irf5
Maf
Akt3
Ralgds
Emp1
Csf1r
Pbx1
Prex1
C)
Lin-
Osteoclast differentiation
Synapse organization
Epithelial cell proliferation
Transcriptional misregulation in cancer
Cell chemotaxis
Sensory perception of sound
Myotome development
Regulation of ion transport
Gland development
Regulation of hemopoiesis
Temperature homeostasis
Second-messenger-mediated signaling
Cytokine-cytokine receptor interaction
Regulation of secretion
PI3K-Akt signaling pathway
Acid secretion
Regulation of growth
Macrophage activation
Regulation of neurotransmitter levels
Cellular response to amyloid-beta
-Log10(P value)
D)
CD11b+
Chemotaxis
Blood vessel morphogenesis
Vesicle-mediated transport
Cell morphogenesis in differentiation
Lipid biosynthetic process
Leukocyte cell-cell adhesion
Positive reg. of response to ext. stim.
Extracellular structure organization
Positive reg. of hydrolase activity
Cellular metal ion homeostasis
Transport of small molecules
Myeloid leukocyte activation
Endocytosis
Regulation of MAPK cascade
Vasculogenesis
Response to wounding
Positive regulation of cell death
Blood circulation
Muscle structure development
Synapse pruning
-Log10(P value)
E)
Lin-
Fold Change
Hoxa9
Hoxa10
Hoxa7
Cd69
Notch1
Csf2rb
WT/MLL-Af4
I3KO/MLL-Af4
F)
CD11b+
Fold Change
Ccnd1
Maf
Mafb
Itga6
Klf4
Akt3
WT/MLL-Af4
I3KO/MLL-Af4
G)
CD11b+
Activation (RLU)
WT
I3KO
WT/MLL-Af4
I3KO/MLL-Af4

Figure 5

Figure 5: IGF2BP3 enhances MLL-Af4 mediated leukemogenesis through targeting transcripts within leukemogenic and Ras signaling pathways.

A) Volcano plot of differentially expressed genes determined using DESeq analysis on RNA-seq samples from WT/MLL-Af4 or I3KO/MLL-Af4 Lin- cells. Dotted lines represent 1.0-fold–change in expression (vertical lines) and adjusted $P < 0.1$ cutoff (horizontal line). IGF2BP3 eCLIP-seq targets are highlighted in red.

B) Volcano plot of differentially expressed transcripts determined using DESeq analysis on RNA-seq samples from WT/MLL-Af4 or I3KO/MLL-Af4 CD11b+ cells. Dotted lines represent 1.0-fold–change in expression (vertical lines) and adjusted $P < 0.1$ cutoff (horizontal line). IGF2BP3 eCLIP-seq targets are highlighted in red.

C) GO Biological Processes and KEGG Pathway enrichment determined utilizing the Metascape enrichment analysis webtool on MLL-Af4 Lin- IGF2BP3 DESeq dataset with an adjusted $P < 0.05$ cutoff.

D) GO Biological Processes and KEGG Pathway enrichment determined utilizing the Metascape enrichment analysis webtool on MLL-Af4 CD11b+ IGF2BP3 DESeq dataset with an adjusted $P < 0.05$ cutoff. Bar graphs are ranked by P value and overlap of terms within gene list.

E) Expression of leukemogenic target genes in WT/MLL-Af4 and I3KO/MLL-Af4 Lin- cells by RT-qPCR (n= 4; t-test; *$P < 0.05$, **$P < 0.01$, ****$P < 0.0001$).

F) Expression of Ras signaling pathway genes in WT/MLL-Af4 and I3KO/MLL-Af4 CD11b+ cells by RT-qPCR (n=4; t-test; *$P < 0.05$, **$P < 0.01$, ***$P < 0.001$).

G) Ras GTPase activity by ELISA in WT/MLL-Af4 and I3KO/MLL-Af4 CD11b+ cells (n=3; t-test; *$P < 0.05$).

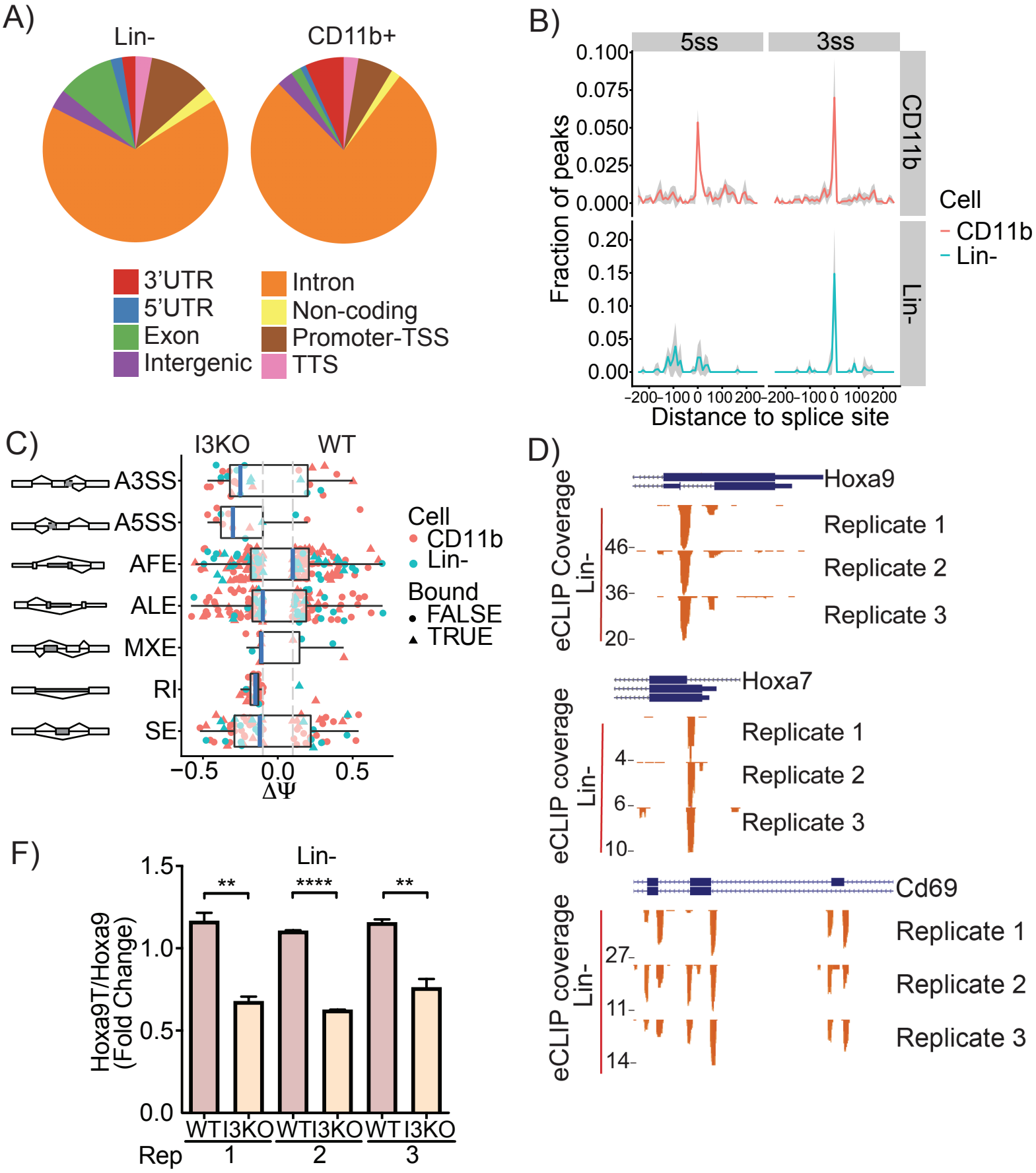
A)
Lin-
CD11b+
3'UTR
5'UTR
Exon
Intergenic
Intron
Non-coding
Promoter-TSS
TTS
B)
5ss
3ss
CD11b
Lin-
Fraction of peaks
Distance to splice site
Cell
CD11b
Lin-
C)
I3KO
WT
A3SS
A5SS
AFE
ALE
MXE
RI
SE
ΔΨ
Cell
CD11b
Lin-
Bound
FALSE
TRUE
D)
Hoxa9
Replicate 1
Replicate 2
Replicate 3
eCLIP Coverage
Lin-
Hoxa7
eCLIP coverage
Cd69
F)
Lin-
Hoxa9T/Hoxa9 (Fold Change)
WT I3KO WT I3KO WT I3KO
Rep 1 2 3

Figure 6

Figure 6: eCLIP analysis reveals IGF2BP3 function in regulating alternative pre-mRNA splicing.

A) Genomic locations of IGF2BP3 eCLIP peaks in WT/MLL-Af4 Lin- cells and CD11b+ cells.

B) Histogram showing normalized IGF2BP3 eCLIP peak counts and distance from IGF2BP3 eCLIP peak of 5' (5ss) and 3' (3ss) splice sites in WT/MLL-Af4 CD11b+ (top) cells and Lin- cells (bottom).

C) Distribution of types of alternative splicing patterns for WT/MLL-Af4 or I3KO/MLL-Af4 Lin- and CD11b+ cells using MISO analysis. Delta psi values plotted indicate difference in isoforms.(A3SS, Alternative 3' splice sites; A5SS, Alternative 5' splice sites; AFE, Alternative first exons; ALE, Alternative last exons; MXE, Mutually exclusive exons; RI, Retained introns; SE, Skipped exons; Bound, IGF2BP3 eCLIP target).

D) UCSC Genome Browser snapshots of the Hoxa9, Hoxa7, and Cd69 loci. Each panel shows the exon-intron structure of the gene and unique read coverage from 3 eCLIP biological replicates from WT/MLL-Af4 Lin- cells. The maximum number of reads at each position is indicated to the left of each histogram.

F) Ratio of Hoxa9T/Hoxa9 isoforms in WT/MLL-Af4 and I3KO/MLL-Af4 Lin- cells by RT-qPCR (t-test; **$P < 0.01$, ****$P < 0.0001$).